

DIFFERENTIATION WITH HIGH-GAIN OBSERVERS
IN THE PRESENCE OF MEASUREMENT NOISE

By

Luma K. Vasiljevic

A THESIS

Submitted to
Michigan State University
in partial fulfillment of the requirements
for the degree of

MASTER OF SCIENCE

Department of Electrical Engineering

2007

ABSTRACT

DIFFERENTIATION WITH HIGH-GAIN OBSERVERS IN THE PRESENCE OF MEASUREMENT NOISE

By

Luma K. Vasiljevic

The error in estimating the derivative(s) of a noisy signal by using a high-gain observer is studied and quantified. The error is bounded in terms of the infinity norms of the noise and a derivative of the signal. The error bound is independent of the frequency or derivatives of the noise. Guidelines are presented for the observer gain design when it is used for on-line differentiation. Analytical and simulation results are presented.

*I dedicate this thesis to my husband Njegovan for
his tremendous support throughout my graduate studies*

ACKNOWLEDGMENTS

I am grateful to my adviser Professor Hassan Khalil for bringing this topic to my attention and for his priceless guidance throughout the research and writing of this thesis.

Contents

List of Figures	vii
List of Tables	ix
1 Introduction	1
1.1 Motivation	2
1.2 Higher Order Sliding Modes	3
1.2.1 The Idea of Sliding-Mode Control	3
1.2.2 First and Second Order Sliding Modes	8
1.3 High Gain Observers	11
1.3.1 Stabilization	16
2 Differentiation with High-Gain Observer in the Presence of Measurement Noise	19
2.1 High-Gain Observer as a Differentiator	20
2.2 The Differentiation Error in the Absence of Noise	22
2.3 The Differentiation Error for Noisy Signals	26
2.4 Computation of the Bound	30
2.5 Conservatism of the Bound	33
2.6 Computer Simulation	35
2.6.1 The Effect of the Eigenvalues and the Order of the Observer on the Error Bound	35
2.6.2 Comparison Between the Actual Estimation Error and the Error Bound	45
3 A Comparison Between High-Gain Observers and Exact Robust Sliding-Mode Differentiators	51
3.1 Robust Exact Differentiation via Sliding Mode Technique	51
3.2 Arbitrary Order Robust Exact Differentiator	54
3.3 In Comparison to High-Gain Observers	58
3.4 Computer Simulation	62
4 Conclusions	72

List of Figures

2.1	The error bound as a function of the high-gain observer parameter ε .	29
2.2	The function $g(t)$.	32
2.3	The gain of the high-gain observer as a function of frequency.	34
2.4	The estimation error as a function of time. The first derivative of a sinusoidal signal is estimated with a second order high-gain observer with $\varepsilon = 0.01$.	39
2.5	The estimation error as a function of time. The derivatives of a sinusoidal signal are estimated with a third order high-gain observer with $\varepsilon = 0.01$.	40
2.6	The estimation error as a function of time. The first derivative of a sinusoidal signal is estimated with a fourth order high-gain observer with $\varepsilon = 0.01$.	41
2.7	The noise $\mu(t)$ in time and frequency domain.	42
2.8	The error bound for the derivatives as a function of ε for a 4 th order high-gain observer with multiple real eigenvalues.	43
2.9	The estimation error as a function of time. The first derivative of a noisy sinusoidal signal is estimated with a 2 nd order high-gain observer. The magnitude of the noise is $\ \mu\ _\infty = 0.012$, $\ u''\ _\infty = 1$, and $\varepsilon = \varepsilon_1^{opt}$.	44
2.10	The estimation error as a function of time. The derivatives of a noisy sinusoidal signal are estimated with a 3 rd order high-gain observer. The magnitude of the noise is $\ \mu\ _\infty = 0.012$, $\ u^{(3)}\ _\infty = 1$, and $\varepsilon = (\varepsilon_1^{opt} + \varepsilon_2^{opt})/2$.	45
2.11	The estimation error as a function of time. The derivatives of a noisy sinusoidal signal are estimated with a 4 th order high-gain observer. The magnitude of the noise is $\ \mu\ _\infty = 0.012$, $\ u^{(4)}\ _\infty = 1$, and $\varepsilon = (\varepsilon_1^{opt} + \varepsilon_2^{opt} + \varepsilon_3^{opt})/3$.	46
2.12	Actual error compared to the error bound (2.12) for estimating the first and second derivative of u as described by (3.4) with a 3 rd order high-gain observer.	48

2.13	Actual error compared to the error bound (2.12) for estimating the first and second derivative of u given by (2.19) with a 3^{rd} order high-gain observer.	49
2.14	Actual error compared to the error bound (2.12) for estimating the first and second derivative of $u(t) = \sin(t)$ with a 3^{rd} order high-gain observer.	50
3.1	Sliding-mode/high-gain estimate of first and second derivative of a noisy sinusoid.	64
3.2	The estimate of derivatives of $\sin(10t) + \mu(t)$ with high-gain/sliding-mode observer. The noise magnitude is $\ \mu\ _\infty = 0.1$	69
3.3	The estimate of derivatives of (3.14) with high-gain/sliding-mode observer. The solid line depicts the actual derivative, whereas the dashed line is the estimate.	70
3.4	Sliding-mode/high-gain estimate of the derivatives of u_1 given by (3.16). The solid line depicts the actual derivative, whereas the dashed line is the estimate.	71

List of Tables

2.1	The constant $\sqrt{Q_2 P_2}$ for $k = 1$ and $n = 2$	36
2.2	The expression $Q_{k+1}^{(1-\frac{k}{n})} P_{k+1}^{k/n}$ for $1 \leq k \leq 2$ and $n = 3$	36
2.3	The expression $Q_{k+1}^{(1-\frac{k}{n})} P_{k+1}^{k/n}$ for $1 \leq k \leq 3$ and $n = 4$	37
2.4	The expression $Q_{k+1}^{(1-\frac{k}{n})} P_{k+1}^{k/n}$ for $1 \leq k \leq 4$ and $n = 5$	38
3.1	A comparative summary of the features of high-gain observers versus robust exact differentiators developed by A. Levant	61
3.2	The percentage differentiation error for a 6^{th} order high-gain observer and a 6^{th} order HOSM differentiator. The differentiated signal is $\sin(t)$ and $\ \mu\ _\infty = 0.01$	63
3.3	The percentage differentiation error for a 6^{th} order high-gain observer and a 6^{th} order HOSM differentiator. The differentiated signal is $\sin(0.5t)$ and $\ \mu\ _\infty = 0.01$	65
3.4	The percentage differentiation error for a 6^{th} order high-gain observer and a 6^{th} order HOSM differentiator. The differentiated signal is $\sin(5t)$ and $\ \mu\ _\infty = 0.01$	65
3.5	The percentage differentiation error for a 6^{th} order high-gain observer and a 6^{th} order HOSM differentiator. The differentiated signal is $\sin(10t)$ and $\ \mu\ _\infty = 0.01$	66
3.6	The percentage differentiation error for a 6^{th} order high-gain observer and a 6^{th} order HOSM differentiator. The differentiated signal is $\sin(50t)$ and $\ \mu\ _\infty = 0.01$	66
3.7	The percentage differentiation error for a 6^{th} order high-gain observer and a 6^{th} order HOSM differentiator. The differentiated signal is $\sin(0.1t)$ and $\ \mu\ _\infty = 0.1$	67
3.8	The percentage differentiation error for a 6^{th} order high-gain observer and a 6^{th} order HOSM differentiator. The differentiated signal is $\sin(t)$ and $\ \mu\ _\infty = 0.1$	67

3.9	The percentage differentiation error for a 6^{th} order high-gain observer and a 6^{th} order HOSM differentiator. The differentiated signal is $\sin(10t)$ and $\ \mu\ _\infty = 0.1$	68
1	The constants P_k for $2 \leq k \leq n$, $2 \leq n \leq 10$ for multiple real eigenvalues	75
2	The constants Q_k for $2 \leq k \leq n$, $2 \leq n \leq 10$ for multiple real eigenvalues	75

Chapter 1

Introduction

Differentiation of signals in real time is an old and well-known problem. An ideal differentiator would have to differentiate measurement noise with possibly large derivatives along with the signal. In [25], the differentiation error for a higher-order sliding mode differentiator is quantified in terms of the magnitude of the noise; that is, a bound on the error is derived that depends on the magnitude of the noise and not its derivative or frequency. Such quantification is useful because it provides insight into the signal to noise ratio of the differentiated signal.

In this thesis we derive a similar bound on the differentiation error when a high-gain observer is used to estimate the derivative(s) of a signal in the presence of measurement noise. The error bound depends on the infinity norm of the noise and the infinity norm of the derivative of the highest estimated derivative of the signal.

Ideally, when no noise is present the error in estimating the derivative with a high-gain observer shrinks to zero as the observer gain grows to infinity. However, large gain undesirably magnifies the measurement noise. There is a trade-off between the closeness of the estimate to the true derivative in the absence of noise and the noise amplification in the presence of noise. This trade-off is studied

and quantified in this thesis. Guidelines are provided for designing the observer gain. Results are illustrated by numerical simulation. Simulation results show that the performance of the high-gain observer with properly designed gain is at least comparable to the performance of the sliding-mode observer in the presence of measurement noise.

1.1 Motivation

In many cases, the differentiation problem is reduced to observation and filtering problems. In the case when the frequency bands of the signal and noise are known, band-pass filters are used to damp noises and the transfer function of the differentiator is approximated by the transfer function of a linear system. When stochastic models for the signal and noise are available, detection and linear filtering theory could be utilized [19], [20], [8]. If no information is available about the bandwidth or stochastic properties of the noise, it is useful to have insight on the accuracy a differentiator could achieve. In [25] A. Levant points out that no differentiator that is exact on input signals whose $(n - 1)^{th}$ derivative has a Lipschitz constant L , producing the i^{th} derivative, where $i < n$, can provide for accuracy better than $L^{i/n} \|\mu\|_{\infty}^{(n-i)/n}$, in the presence of uniformly bounded noise $\mu(t)$ ¹. Indeed, being exact on signals whose $(n - 1)^{th}$ derivative has a Lipschitz constant L , the differentiator must be exact on sinusoidal noise with amplitude $\|\mu\|_{\infty}$ and frequency $(L/\|\mu\|_{\infty})^{1/n}$, producing an error of at least $L^{i/n} \|\mu\|_{\infty}^{(n-i)/n}$ in the presence of noise. That is, a second-order differentiator exact in the absence of noise on signals whose first derivative have Lipschitz constant L , must make an error that is at least $\sqrt{L/\|\mu\|_{\infty}}$ in the presence of uniformly bounded measurement noise $\mu(t)$. In [25] and [24] A. Levant proposes

¹ $\|\mu\|_{\infty} = \sup_{t>0} |\mu(t)|$

differentiators that compute the i^{th} derivative exactly for signals whose $(n-1)^{th}$ derivative has Lipschitz's constant L in the absence of noise and produce an error bounded by $KL^{i/n}\|\mu\|_{\infty}^{(n-i)/n}$, for some $K > 0$, in the presence of noise. Levant's differentiators utilize Higher Order Sliding Modes (HOSM).

In this thesis, we show analytically that the same accuracy could be achieved with high-gain observers in the presence of noise, given the appropriate choice of the observer gain. We utilized computer simulation to demonstrate our results and compare the performance of HOSM observers and high-gain observers in the presence of measurement noise. In this chapter, we briefly review the concepts and ideas of HOSM and high-gain observers omitting formal proofs. We refer the reader to appropriate sources for the formal theories. In Chapter 2, we show how the high-gain observer could be used as a differentiator in the presence of measurement noise, whereas Chapter 3 is a comparison between HOSM differentiators and high-gain observer-based differentiators. Finally, Chapter 4 is a brief summary of results presented in this thesis.

1.2 Higher Order Sliding Modes

1.2.1 The Idea of Sliding-Mode Control

An obvious way to achieve a control task under heavy uncertainty conditions is to keep some constraints by "brute force." The most simple way to keep an equality constraint is to react immediately to any deviation of the system stirring it back to the constraint by sufficiently energetic effort. This approach leads to so-called sliding modes [18]. To illustrate this idea, we present the following example.

Example – Stabilization Utilizing Sliding Mode

For the system (1.1) in regular form [22]

$$\begin{aligned}\dot{\eta} &= f_a(\eta, \xi), \\ \dot{\xi} &= f_b(\eta, \xi) + g(\eta, \xi)u + \delta(t, \eta, \xi, u),\end{aligned}\tag{1.1}$$

where² $x = (\eta, \xi) \in R^2$ is the state, $u \in R$ is the control input, f_a , f_b and g are sufficiently smooth functions in a domain $D \subset R^2$ that contains the origin. We assume that f_a and f_b are known, whereas g and δ are uncertain. We also assume that g is positive and bounded away from zero; that is $g \geq g_0 > 0$. The function δ is piecewise continuous in t and sufficiently smooth in (η, ξ, u) for $(t, \eta, \xi, u) \in [0, \infty) \times D \times R$. Suppose that in the absence of δ the origin is an open-loop equilibrium point. Our goal is to design a state feedback control law to stabilize the origin for all uncertainties in g and δ .

We begin by designing the sliding manifold (constraint) $s = \xi - \phi(\eta) = 0$ such that when motion is restricted to the manifold, the reduced-order model

$$\dot{\eta} = f_a(\eta, \phi(\eta))$$

has an asymptotically stable equilibrium point at the origin. The design of $\phi(\eta)$ amounts to solving a stabilization problem for the system

$$\dot{\eta} = f_a(\eta, \xi)$$

with ξ viewed as the control input. We assume that we can find a stabilizing continuously differentiable function $\phi(\eta)$ with $\phi(0) = 0$. Next, we design u to

²For simplicity, we consider a single-input 2^{nd} order system. See [22] for multi-input higher-order system.

bring s to zero in finite time and maintain it there for all future time. Toward that end, we write the \dot{s} equation:

$$\dot{s} = f_b(\eta, \xi) - \frac{\partial \phi}{\partial \eta} f_a(\eta, \xi) + g(\eta, \xi)u + \delta(t, \eta, \xi, u) \quad (1.2)$$

In the absence of uncertainty; that is, when $\delta = 0$ and g is known, taking $u = -g^{-1} [f_b - (\partial\phi/\partial\eta)f_a]$ results in $\dot{s} = 0$, which ensures that the condition $s = 0$ can be maintained for all future time. Assume that

$$\left| \frac{f_b(x) - \frac{\partial \phi}{\partial \eta} f_a(x) + \delta(t, x, u)}{g(x)} \right| \leq \rho(x) + k_0 \|u\|_\infty, \forall (t, \eta, \xi, v) \in [0, \infty) \times D \times R, \quad (1.3)$$

where the continuous function $\rho(x) \geq 0$ and $k_0 \in [0, 1)$ are known. Utilizing $V = (1/2)s^2$ as a Lyapunov function candidate for (1.2), we obtain

$$\dot{V} = s\dot{s} = sg(x)u + s[f_b(x) - \frac{\partial \phi}{\partial \eta} f_a(x) + \delta(t, x, u)] \leq g(x) \{su + |s|[\rho(x) + k_0|u|]\}.$$

Take

$$\dot{u} = -\beta(x)\text{sign}(s), \quad (1.4)$$

where

$$\beta(x) \geq \frac{\rho(x)}{1 - k_0} + \beta_0, \quad \forall (x) \in D \quad (1.5)$$

and $\beta_0 > 0$. Then,

$$\begin{aligned} \dot{V} &\leq g(x)[- \beta(x) + \rho(x) + k_0\beta(x)]|s| = g(x)[-(1 - k_0)\beta(x) + \rho(x)]|s| \\ &\leq g(x)[- \rho(x) - (1 - k_0)\beta_0 + \rho(x)]|s| \leq -g_0(x)\beta_0(1 - k_0)|s|. \end{aligned}$$

The inequality $\dot{V} \leq -g_0(x)\beta_0(1 - k_0)|s|$ ensures that all trajectories starting off

the manifold $s = 0$ reach it in finite time and those on the manifold cannot leave it.

Higher order sliding modes (HOSM) generalize the basic sliding mode idea acting on the higher order time derivatives of the system deviation from the constraint instead of influencing the first deviation derivative as it happens in standard sliding modes. A number of such controllers were described in the literature [6, 7, 13, 26, 28]. HOSM is a movement on a discontinuity set of a dynamic system understood in Filippov sense [17]. The sliding order characterizes the dynamic smoothness degree in the vicinity of the mode. If the task is to provide for keeping a constraint given by equality of a smooth function s to zero, the sliding order is the number of continuous total derivatives of s (including the zero one) in the vicinity of the sliding mode. Hence, the r^{th} order sliding mode is determined by the equalities

$$s = \dot{s} = \ddot{s} = \dots = s^{(r-1)} = 0$$

forming an r -dimensional condition on the state of the dynamic system. The words “ r^{th} order sliding” are often abridged to “ r -sliding.”

Real Sliding vs. Ideal Sliding

For the smooth time-varying dynamic system described by the equation

$$\dot{x} = f(t, x, u), \tag{1.6}$$

where x is a state variable that takes values on a smooth manifold X , t is time and $u \in R^m$ is control. The design objective is the synthesis of a control u such that the constraint $s(t, x) = 0$ holds. Here, $s : R \times X \rightarrow R^m$ and both f and s are smooth enough mappings. A motion that takes place strictly on

the constraint manifold $s = 0$ is called an *ideal sliding* [26]. We also informally call every motion in a small neighborhood of the constraint manifold a *real sliding* [32, 33]. The 1st-order sliding mode (as in example above) exists due to infinite frequency of the control switching. However, due to switching imperfections this frequency is finite. The sliding mode notion should be understood as a limit of motions when switching imperfections vanish and the switching frequency tends to infinity [17, 1, 2]. The definitions below were introduced in [26].

Definition 1 Let $(t, x(t, \varepsilon))$ be a family of trajectories indexed by $\varepsilon \in R$ with common initial condition $(t_0, x(t_0))$ and let $t \geq t_0$ (or $t \in [t_0, T]$). Assume that there exists $t_1 \geq t_0$ (or on $[t_0, T]$) such that on every segment $[t', t'']$, where $t' \geq t_1$ (or on $[t_1, T]$) the function $s(t, x(t, \varepsilon))$ tends uniformly to zero with ε tending to zero. In this case we call such a family a *real sliding family* on the constraint $s = 0$. We call the motion on the interval $[t_1, \infty)$ (or $[t_1, T]$) a *steady state process*.

The term *control algorithm* is used for a rule to form the control signal [26].

Definition 2 A control algorithm is called an *ideal sliding algorithm* on the constraint $s = 0$ if it yields an ideal sliding in finite time for every initial condition.

Definition 3 A control algorithm depending on a parameter $\varepsilon \in R$ is called a *real sliding algorithm* on the constraint $s = 0$ if with $\varepsilon \rightarrow 0$, it forms a *real sliding family* for every initial condition.

1.2.2 First and Second Order Sliding Modes

Preliminaries

For the closed loop control system

$$\dot{x} = f(t, x, u) \quad (1.7)$$

$$u = U(t, x, \xi) \quad (1.8)$$

$$\dot{\xi} = \psi(t, x, \xi) \quad (1.9)$$

where U is a feedback operator, ξ is a special auxiliary parameter ('operator variable' as in [12, 11]). The initial value of ξ may be defined as a special function $\xi(t_0) = \xi_0(t_0, x_0)$ or considered to be arbitrary. Equations (1.8) and (1.9) constitute what is called a binary control algorithm [11, 12]. Let $s(t, x)$ be the desirable constraint, with $s \in C^1$, and $\partial s / \partial x \neq 0$.

Definition 4 *Equations (1.8)/(1.9) are called the first/second order sliding algorithm on the constraint $s = 0$ if a stable sliding mode of the first/second order on the manifold $s = 0$ is achieved, and for every initial condition (t_0, x_0) the state x is transferred to the sliding manifold in finite time.*

First order sliding is characterized by a piecewise continuous function U and $\psi = 0$. The second order sliding algorithms are given by a continuous function U and a bounded discontinuous function ψ , therefore, the sliding problem is solved by means of a continuous control [29, 30, 31, 13, 14, 15, 16].

For simplicity, we take $s \in R, u \in R$ and $t, s(t), u(t)$ available. The goal is to force the constraint $s(t)$ to vanish. Assume the conditions:

1. In (1.7) the function f is C^1 . The function s is C^2 . We assume that $x \in X$, where X is a smooth finite-dimensional manifold. Any solution of

(1.7) is well defined for all t provided that the control $u(t)$ is continuous and satisfies $|u(t)| \leq \rho < 1$ for each t .

2. Assume there exists $u_1 \in (0, 1)$ such that for any continuous function u , $|u| > u_1$, implies $su > 0$.

Remark: This condition implies that there is at least one t such that $s(t) = 0$ provided u has a certain structure. Consider the differential operator

$$L_u(\cdot) = \frac{\partial}{\partial t}(\cdot) + \frac{\partial}{\partial x}(\cdot)f(t, x, u)$$

where L_u is the total derivative with respect to (1.7) when u is considered a constant. Define \dot{s} as

$$\dot{s}(t, x, u) = L_u s(t, x) = s'_t(t, x) + s'_x(t, x)f(t, x, u)$$

3. There are positive constants s_0, K_M, K_m and $u_0 < 1$, such that $|s(t, x)| < s_0$ implies

$$0 < K_m \leq \frac{\partial \dot{s}}{\partial u} \leq K_M$$

for all u , whereas the inequality $|u| > u_0$ implies $\dot{s}u > 0$.

4. The set $\{t, x, u : |s(t, x)| < s_0\}$ is called the linearity region. There is a constant C_0 such that in the linearity region the inequality $|L_u L_u s(t, x)| < C_0$ holds.
5. The region $|s| \leq s_0 - \delta$, where $0 < \delta < s_0$ is called the reduced linearity region.

Sliding Algorithms

The algorithm

$$u = \begin{cases} -signs & \text{with } |s/\varepsilon| > 1 \\ -s/\varepsilon & \text{with } |s/\varepsilon| \leq 1 \end{cases},$$

forms a real sliding algorithm of the first order.

For $\alpha_M > \alpha_m > 0, \alpha_m > 4K_M/s_0, \alpha_m > C_0/K_m$, and $K_m\alpha_M - C_0 > K_M\alpha_m + C_0$, the "twisting algorithm" (below) is a second order sliding algorithm [13, 14, 29]

$$\dot{u} = \begin{cases} -u & \text{with } |u| > 1 \\ -\alpha_m signs & \text{with } s\dot{s} \leq 0, |u| \leq 1 \\ -\alpha_M signs & \text{with } s\dot{s} > 0, |u| \leq 1 \end{cases},$$

The algorithm (prescribed law of variation of s [13])

$$\dot{s} = \begin{cases} -u & \text{for } |u| > 1 \\ -\alpha sign(\dot{s} - g(s)), & \text{for } |u| \leq 1 \end{cases},$$

constitutes a second-order sliding algorithm on the constraint $s = 0$, provided that $\alpha > 0$ is sufficiently large and the initial conditions are within the reduced linearity region. The function $g(s)$ is smooth everywhere except on $s = 0$. Also, all solutions of the equation $\dot{s} = g(s)$ vanish in a finite time and that the function $\dot{g}(s)g(s)$ is bounded. For example, with $\lambda > 0$ and $0.5 \leq \gamma < 1, g(s) = -\lambda signs|s|^\gamma$, may be used.

All the above examples of sliding algorithms use the derivatives of s calculated with respect to the system. The following is an example that does not utilize this property [16]. For $\alpha, \lambda > 0, 0 < \rho \leq 1/2, \alpha > C_0/K_m, \alpha > 4K_M/s_0, \rho(\lambda K_m)^{1/\rho} >$

$(K_M\alpha + C_0)(2K_M)^{1/\rho-2}$ and $|u(t_0)| \leq \rho$, the algorithm

$$u = u_1 + u_2, \quad (1.10)$$

$$\dot{u}_1 = \begin{cases} -u & \text{for } |u| > 1 \\ -\alpha \text{signs} & \text{for } |u| \leq 1 \end{cases}, \quad (1.11)$$

$$u_2 = \begin{cases} -\lambda|s_0|^\rho \text{signs} & \text{for } |s| > s_0 \\ -\lambda|s|^\rho \text{signs} & \text{for } |s| \leq s_0 \end{cases}, \quad (1.12)$$

constitutes a second-order sliding on $s = 0$.

In [25] Levant describes arbitrary order sliding algorithms. These algorithms use the derivatives of the output to achieve higher order sliding. He also develops exact, robust differentiators based on algorithm (1.10), (1.11) and (1.12) that provide derivatives of arbitrary order. In Chapter 3 we review the robust, exact differentiators developed by Levant and then compare them to high-gain observers.

1.3 High Gain Observers

In many practical problems we cannot measure all state variables due to technical or economical reasons. Therefore, we have to use dynamic compensation to extend state feedback designs to output feedback. One form of dynamic compensation is to use observers that asymptotically estimate the states from output measurements. High-gain observers guarantee that the output feedback controller recovers the performance of the state feedback controller when the observer gain is sufficiently high. The *separation principle* allows us to separate the design into two

tasks. First, we design a state feedback controller that stabilizes the system and meets other design specifications. Then, we design an output feedback controller replacing the state x by its estimate \hat{x} provided by the high-gain observer. A key property that makes this separation possible is the design of the state feedback controller to be globally bounded in x . High-gain observers are robust to model uncertainties and can be used in a wide range of control problems [22, 21].

Example

Consider the second-order nonlinear system [22]

$$\begin{aligned}\dot{x}_1 &= x_2 \\ \dot{x}_2 &= \phi(x, u) \\ y &= x_1\end{aligned}\tag{1.13}$$

where $x = [x_1, x_2]^T$. Suppose $u = \gamma(x)$ is locally Lipschitz state feedback control law that stabilizes the origin $x = 0$ of the closed loop system

$$\begin{aligned}\dot{x}_1 &= x_2 \\ \dot{x}_2 &= \phi(x, \gamma(x))\end{aligned}\tag{1.14}$$

To implement this feedback control using only measurement of the output y , we use the observer

$$\begin{aligned}\dot{\hat{x}}_1 &= \hat{x}_2 + h_1(y - \hat{x}_1) \\ \dot{\hat{x}}_2 &= \phi_0(x, u) + h_2(y - \hat{x}_1)\end{aligned}\tag{1.15}$$

where $\phi_0(x, u)$ is a nominal model of the nonlinear function $\phi(x, u)$. The estimation error

$$\tilde{x} = \begin{bmatrix} \tilde{x}_1 \\ \tilde{x}_2 \end{bmatrix} = \begin{bmatrix} x_1 - \hat{x}_1 \\ x_2 - \hat{x}_2 \end{bmatrix},$$

satisfies the equation

$$\begin{aligned}\dot{\tilde{x}}_1 &= -h_1\tilde{x}_1 + \tilde{x}_2 \\ \dot{\tilde{x}}_2 &= -h_2\tilde{x}_1 + \delta(x, \tilde{x})\end{aligned}\tag{1.16}$$

where $\delta(x, \tilde{x}) = \phi(x, \gamma(\hat{x}))$. We want to design the observer gain $H = [h_1, h_2]^T$ such that $\lim_{t \rightarrow \infty} \tilde{x} = 0$. In the absence of the disturbance term δ , asymptotic error convergence is achieved by designing H such that

$$A_0 = \begin{bmatrix} -h_1 & 1 \\ -h_2 & 0 \end{bmatrix}$$

is Hurwitz. For this second-order system, A_0 is Hurwitz for any positive constants h_1 and h_2 . In the presence of δ we need to design H with the goal of rejecting the effect of δ on \tilde{x} . This is achieved, for any δ , if the transfer function

$$G_0(s) = \frac{1}{s^2 + h_1s + h_2} \begin{bmatrix} 1 \\ s + h_1 \end{bmatrix}$$

from δ to \tilde{x} is identically 0. While this is not possible, we can make $\sup_{\omega \in R} |G_0(j\omega)|$ arbitrarily small by choosing $h_2 \gg h_1 \gg 1$. In particular, taking

$$h_1 = \frac{\alpha_1}{\varepsilon}, \quad h_2 = \frac{\alpha_2}{\varepsilon^2}\tag{1.17}$$

for some positive constants α_1, α_2 and ε , with $\varepsilon \ll 1$, it can be shown that

$$G_0(s) = \frac{\varepsilon}{(\varepsilon s)^2 + \varepsilon\alpha_1s + \alpha_2} \begin{bmatrix} \varepsilon \\ \varepsilon s + \alpha_1 \end{bmatrix}.$$

Hence, $\lim_{\varepsilon \rightarrow 0} G_0(s) = 0$. The disturbance rejection property of the high-gain observer can be also seen in the time domain by representing the error equation 1.16 in the singularly perturbed form. Toward that end, define the scaled estimation

errors

$$\eta_1 = \frac{\tilde{x}_1}{\varepsilon}, \quad \eta_2 = \tilde{x}_2. \quad (1.18)$$

The newly defined variables satisfy the singularly perturbed equation

$$\begin{aligned} \varepsilon \dot{\eta}_1 &= -\alpha_1 \eta_1 + \eta_2, \\ \varepsilon \dot{\eta}_2 &= -\alpha_2 \eta_2 + \varepsilon \delta(x, \tilde{x}). \end{aligned} \quad (1.19)$$

This equation shows clearly that reducing ε diminishes the effect of δ . It shows also that, for small ε , the scaled-estimation error η will be much faster than x . Notice, however, that $\eta_1(0)$ will be $O(1/\varepsilon)$ whenever $x_1(0) \neq \hat{x}_1(0)$. Consequently, the solution of (1.19) will contain a term of the form $(1/\varepsilon)e^{-at/\varepsilon}$ for some $a > 0$. Whereas this exponential mode decays rapidly, it exhibits an impulsive-like behavior where the transient peaks to $O(1/\varepsilon)$ values before it decays rapidly toward zero. In fact, the function $(a/\varepsilon)e^{-at/\varepsilon}$ approaches an impulse function as ε tends to zero. This behavior is known as the *peaking phenomenon*. It is important to realize that the peaking phenomenon is not a consequence of using the change of variables (1.18) to represent the error dynamics in the singularly perturbed form. It is an intrinsic feature of any high-gain observer with $h_2 \gg h_1 \gg 1$. Fortunately, we can overcome the peaking phenomenon by saturating the control outside a compact region of interest to create a buffer that protects the plant from peaking [22].

The full-order observer (1.15) provides estimates (\hat{x}_1, \hat{x}_2) that are used to replace (x_1, x_2) in the feedback control law. Since $y = x_1$ is measured, we can use x_1 in the control law and only replace x_2 by \hat{x}_2 . Furthermore, we can use

the reduced-order observer

$$\begin{aligned}\dot{w} &= -h(w + hy) + \phi_0(\hat{x}, u) \\ \hat{x}_2 &= w + hy\end{aligned}\tag{1.20}$$

where $h = \alpha/\varepsilon$ for some positive constants α and ε with $\varepsilon \ll 1$, to estimate \hat{x}_2 . The reduced-order high-gain observer (1.20) exhibits the peaking phenomenon as the full-order observer and is remedied by saturating the control as well.

The high-gain observer is basically an approximate differentiator. When ϕ_0 is chosen to be zero, the high-gain observer is linear. The transfer function for the full-order observer from y to \hat{x} is

$$\frac{\alpha_2}{(\varepsilon s)^2 + \alpha_1 \varepsilon s + \alpha_2} \begin{bmatrix} 1 + (\varepsilon \alpha_1 / \alpha_2) s \\ s \end{bmatrix} \rightarrow \begin{bmatrix} 1 \\ s \end{bmatrix} \text{ as } \varepsilon \rightarrow 0.$$

For the reduced-order observer the transfer function transfer function from y to \hat{x}_2 is

$$\frac{s}{(\varepsilon/\alpha)s + 1} \rightarrow s \text{ as } \varepsilon \rightarrow 0.$$

Thus, on a compact frequency interval, the high-gain observer approximates \dot{y} for sufficiently small ε . Realizing that the high-gain observer is an approximate differentiator we can see that measurement noise and unmodeled high-frequency sensor dynamics will put a practical limit on how small ε could be. Examples of application to induction motors and mechanical systems are given in [4, 9, 5]. It is for the first time in [23] and this thesis that this limitation is quantified. Guidelines are provided for the choice of ε . This choice takes into account the amplitude of the noise, but it is independent of the frequency of the noise.

1.3.1 Stabilization

Consider the multi-input-multi-output system [22]

$$\begin{aligned}
 \dot{x} &= Ax + B\phi(x, z, u) \\
 \dot{z} &= \psi(x, z, u) \\
 Y &= Cx \\
 \zeta &= q(x, z)
 \end{aligned} \tag{1.21}$$

where $u \in R^p$ is the control input, $y \in R^m$ and $\zeta \in R^s$ are measured outputs, and $x \in R^\rho$ and $z \in R^l$ constitute the state vector. The $\rho \times \rho$ matrix A , the $\rho \times m$ matrix B , and the $m \times \rho$ matrix C are given by

$$\begin{aligned}
 A &= \text{block diag}[A_1, A_2, \dots, A_m], \quad A_i = \begin{bmatrix} 0 & 1 & \dots & \dots & 0 \\ 0 & 0 & 1 & \dots & 0 \\ \vdots & & & \ddots & \vdots \\ 0 & \dots & \dots & 0 & 1 \\ 0 & \dots & \dots & \dots & 0 \end{bmatrix}_{\rho_i \times \rho_i} \\
 B &= \text{block diag}[B_1, B_2, \dots, B_m], \quad B_i = \begin{bmatrix} 0 \\ 0 \\ \vdots \\ 0 \\ 1 \end{bmatrix}_{\rho_i \times 1} \\
 C &= \text{block diag}[C_1, C_2, \dots, C_m], \quad C_i = [1 \ 0 \ \dots \ \dots \ 0]_{1 \times \rho_i}
 \end{aligned}$$

where $1 \leq i \leq m$ and $\rho = \rho_1 + \dots + \rho_m$, represent m chains of integrators. The functions Φ, Ψ and q are locally Lipschitz in their arguments for $(x, z, u) \in D_x \times D_z \times R^p$, where $D_x \subset R^\rho$ and $D_z \subset R^l$ are domains that contain their respective origins. Moreover, $\phi(0, 0, 0) = 0$, $\psi(0, 0, 0) = 0$, and $q(0, 0) =$

0. Our goal is to design an output feedback controller to stabilize the origin. The separation principle (see [22]) allows us to approach the design of the output feedback controller in two steps. First, a partial state feedback controller that uses measurements of x and ζ is designed to asymptotically stabilize the origin. Then, a high-gain observer is used to estimate x from y . The state feedback controller is allowed to be a dynamical system of the form

$$\begin{aligned}\dot{\vartheta} &= \Gamma(\vartheta, x, \zeta) \\ u &= \gamma(\vartheta, x, \zeta)\end{aligned}\tag{1.22}$$

where γ and Γ are locally Lipschitz functions in their arguments over the domain of interest and globally bounded functions of x . Moreover, $\gamma(0, 0, 0) = 0$ and $\Gamma(0, 0, 0) = 0$. For convenience, we write the closed-loop system under state feedback as

$$\dot{\chi} = f(\chi)\tag{1.23}$$

where $\chi = (x, z, \vartheta)$. The output feedback controller is taken as

$$\begin{aligned}\dot{\vartheta} &= \Gamma(\vartheta, \hat{x}, \zeta) \\ u &= \gamma(\vartheta, \hat{x}, \zeta)\end{aligned}\tag{1.24}$$

where \hat{x} is generated by the high-gain observer

$$\dot{\hat{x}} = A\hat{x} + B\phi_0(\hat{x}, \zeta, u) + H(y - C\hat{x})\tag{1.25}$$

The observer gain H is chosen as

$$H = \text{block diag}[H_1, H_2, \dots, H_m], \quad H_i = \begin{bmatrix} \alpha_1^i/\varepsilon \\ \alpha_2^i/\varepsilon^2 \\ \vdots \\ \alpha_{\rho_i-1}^i/\varepsilon^{\rho_i-1} \\ \alpha_{\rho_i}^i/\varepsilon^{\rho_i} \end{bmatrix}_{\rho_i \times 1}$$

where ε is a positive constant to be specified and the constants α_j^i are chosen such that

$$s^{\rho_i} + \alpha_1^i s^{\rho_i-1} + \dots + \alpha_{\rho_i-1}^i s + \alpha_{\rho_i}^i$$

is Hurwitz. The function $\phi_0(x, z, u)$ is a nominal model of $\phi(x, z, u)$ that is locally Lipschitz in its arguments over the domain of interest, globally bounded in x , and $\phi_0(0, 0, 0) = 0$.

Chapter 2

Differentiation with High-Gain Observer in the Presence of Measurement Noise

In this chapter we quantify the differentiation error when a high-gain observer is used as a differentiator, and provide guidelines for the design of the observer's gain and eigenvalues. First, we show how the high-gain observer acts as a differentiator in the limit as the gain approaches infinity. Next, we identify two additive components to the differentiation error in the presence of measurement noise. One component is due to the differentiated signal, whereas the other component is due to measurement noise. We then show that both components are bounded once the gain is chosen. However, the component due to the signal is inversely proportional to a power of the gain, whereas the component due to measurement noise is directly proportional to a power of the gain. Hence, reducing one component increases the other. We show that there exists a gain at which the error is proportional to a power of the ratio of the Lipschitz constant of the derivative of the signal to the magnitude of the noise. We then provide an algorithm to compute the error bound

as a function of the gain, show that there exists a signal for which the bound is realized, and compute the gain for which the error bound is minimized. Finally, we show via simulation how the error for actual signals corrupted with noise relates to the error bound.

2.1 High-Gain Observer as a Differentiator

The linear high-gain observer

$$\begin{aligned}\dot{\hat{x}}_i &= \hat{x}_{i+1} + \left(\frac{\alpha_i}{\varepsilon^i}\right)(y - \hat{x}_1), \quad 1 \leq i \leq n-1 \\ \dot{\hat{x}}_n &= \frac{\alpha_n}{\varepsilon^n}(y - \hat{x}_1).\end{aligned}$$

was developed to estimate the states of a system of the form

$$\begin{aligned}\dot{x}_i &= x_{i+1}, \quad 1 \leq i \leq n-1 \\ \dot{x}_n &= f(x, t) \\ y &= x_1,\end{aligned}\tag{2.1}$$

from its output y , where f is locally Lipschitz in its argument over a domain that contains the origin and $f(0,0) = 0$. Asymptotically, as $\varepsilon \rightarrow 0$, the estimation error $x_i - \hat{x}_i \rightarrow 0$ (see [22, ch. 14]). For $f(x, t) = u^{(n)}$, the states of (2.1) become the derivatives $u^{(i)}, 0 \leq i \leq n-1$, of the input u , whereas the output is $y = x_1 = u$. Thus, the high-gain observer can be represented by

$$\dot{\hat{x}} = \hat{A}\hat{x} + \hat{B}u,\tag{2.2}$$

with

$$\hat{A} = \begin{bmatrix} -\alpha_1/\varepsilon & 1 & \cdots & \cdots & 0 \\ -\alpha_2/\varepsilon^2 & 0 & 1 & \cdots & 0 \\ \vdots & & & \ddots & \vdots \\ -\alpha_{n-1}/\varepsilon^{n-1} & \cdots & \cdots & 0 & 1 \\ -\alpha_n/\varepsilon^n & \cdots & \cdots & \cdots & 0 \end{bmatrix},$$

$$\hat{B} = \begin{bmatrix} \alpha_1/\varepsilon \\ \alpha_2/\varepsilon^2 \\ \vdots \\ \alpha_{n-1}/\varepsilon^{n-1} \\ \alpha_n/\varepsilon^n \end{bmatrix},$$

where the polynomial $s^n + \alpha_1 s^{n-1} + \cdots + \alpha_{n-1} s + \alpha_n$ is Hurwitz. The transfer function from u to \hat{x} is

$$T(s) = \frac{\alpha_n}{p_n(s)} \begin{bmatrix} 1 + \varepsilon \phi_1(\alpha_1, \cdots, \alpha_n, s, \varepsilon) \\ s + \varepsilon \phi_2(\alpha_1, \cdots, \alpha_n, s, \varepsilon) \\ \vdots \\ s^{n-2} + \varepsilon \phi_{n-1}(\alpha_1, \cdots, \alpha_n, s, \varepsilon) \\ s^{n-1} + \varepsilon \phi_n(\alpha_1, \cdots, \alpha_n, s, \varepsilon) \end{bmatrix},$$

where $p_n(s) = \varepsilon^n s^n + \varepsilon^{n-1} \alpha_1 s^{n-1} + \cdots + \varepsilon \alpha_{n-1} s + \alpha_n$ and $\phi_k(\alpha_1, \cdots, \alpha_n, s, \varepsilon)$ for $1 \leq k \leq n$ are polynomials. Thus, in the limit $T(s) \rightarrow [1 \ s \ \cdots \ s^{n-2} \ s^{n-1}]^T$ as $\varepsilon \rightarrow 0$. Hence, asymptotically, as $\varepsilon \rightarrow 0$, system (2.2) acts as a differentiator.

2.2 The Differentiation Error in the Absence of Noise

For the chain of integrators

$$\dot{x} = Ax + Bu^{(n)}, \quad (2.3)$$

with

$$A = \begin{bmatrix} 0 & 1 & \cdots & \cdots & 0 \\ 0 & 0 & 1 & \cdots & 0 \\ \vdots & & & \ddots & \vdots \\ 0 & \cdots & \cdots & 0 & 1 \\ 0 & \cdots & \cdots & \cdots & 0 \end{bmatrix}, \quad B = \begin{bmatrix} 0 \\ 0 \\ \vdots \\ 0 \\ 1 \end{bmatrix}$$

and state vector

$$x = \begin{bmatrix} u \\ u' \\ \vdots \\ u^{(n-2)} \\ u^{(n-1)} \end{bmatrix},$$

the n^{th} order observer that estimates the states is given by (2.2). Consider the scaled estimation error equation

$$\dot{\eta} = \frac{1}{\varepsilon} A \eta - Bu^{(n)}, \quad (2.4)$$

where

$$\eta = \begin{bmatrix} \eta_1 \\ \eta_2 \\ \vdots \\ \eta_{n-1} \\ \eta_n \end{bmatrix} = \begin{bmatrix} \frac{(x_1 - \hat{x}_1)}{\varepsilon^{n-1}} \\ \frac{(x_2 - \hat{x}_2)}{\varepsilon^{n-2}} \\ \vdots \\ \frac{(x_{n-1} - \hat{x}_{n-1})}{\varepsilon} \\ (x_n - \hat{x}_n) \end{bmatrix} = \begin{bmatrix} \frac{(u - \hat{x}_1)}{\varepsilon^{n-1}} \\ \frac{(u' - \hat{x}_2)}{\varepsilon^{n-2}} \\ \vdots \\ \frac{(u^{(n-2)} - \hat{x}_{n-1})}{\varepsilon} \\ (u^{(n-1)} - \hat{x}_n) \end{bmatrix}$$

and

$$A\eta = \begin{bmatrix} -\alpha_1 & 1 & \cdots & \cdots & 0 \\ -\alpha_2 & 0 & 1 & \cdots & 0 \\ \vdots & & & \ddots & \vdots \\ -\alpha_{n-1} & \cdots & \cdots & 0 & 1 \\ -\alpha_n & \cdots & \cdots & \cdots & 0 \end{bmatrix}.$$

In order to show that the ultimate bound on η_k in steady-state, for $1 \leq k \leq n$, is of the order $O\left(\varepsilon \left\|u^{(n)}\right\|_{\infty}\right)$, where $\|u^{(n)}\|_{\infty} = \sup_{t \geq 0} |u^{(n)}(t)|$, we prove the following lemma.

Lemma 1 *Consider the stable linear time-invariant single-input system*

$$\dot{z} = Mz + Nw, \quad (2.5)$$

where M is Hurwitz and $\|z(0)\| \leq a$. Let

$$K_k = \int_0^{\infty} |\{\exp(M\tau)N\}_k| d\tau,$$

for $1 \leq k \leq n$, where $\{.\}_k$ is the k^{th} component of an n -dimensional vector.

Then

1. For all bounded piecewise signals w with $\|w\|_{\infty} \leq c$ and each $1 \leq k \leq n$, z_k is globally uniformly ultimately bounded by¹ $\delta + K_k\|w\|_{\infty}$ where δ could be arbitrarily small²; that is, there is time $T = T(a, c, \delta)$ such that

$$|z_k(T)| \leq K_k\|w\|_{\infty} + \delta, \quad \forall t \geq T$$

2. There is a piecewise continuous w with $\|w\|_{\infty} \leq c$, dependent on k and

¹Throughout this thesis δ denotes an arbitrarily small quantity

²If $z(0) = 0$, then $\delta = 0$

δ , such that

$$|z_k(T)| \geq K_k \|w\|_\infty - \delta.$$

Proof: The solution to (2.5) as a function of time t is given by

$$z(t) = \exp(Mt)z(0) + \int_0^t \exp(M(t-\sigma))Nw(\sigma) d\sigma. \quad (2.6)$$

Since M is Hurwitz,

$$\lim_{t \rightarrow \infty} \{\exp(Mt)z(0)\}_k = 0, \text{ for } 1 \leq k \leq n.$$

For arbitrarily small δ , there is T large enough that $|\{\exp(Mt)z(0)\}_k| \leq \delta$ for $t \geq T$. Hence,

$$\begin{aligned} |z_k(t)| &\leq \delta + \left| \int_0^t \{\exp(M(t-\sigma))N\}_k w(\sigma) d\sigma \right| \\ &\leq \delta + \|w\|_\infty \int_0^t |\{\exp(M(t-\sigma))N\}_k| d\sigma, \\ &= \delta + K_k \|w\|_\infty. \end{aligned} \quad (2.7)$$

On the other hand,

$$\left| z_k(T) - \int_0^T \{\exp(M(T-\sigma))N\}_k w(\sigma) d\sigma \right| \leq \delta.$$

Using the inequality $||a| - |b|| \leq |a - b|$, we have

$$\left| |z_k(T)| - \left| \int_0^T \{\exp(M(T-\sigma))N\}_k w(\sigma) d\sigma \right| \right| \leq \delta.$$

Substituting $\tau = T - \sigma$, we get

$$\left| |z_k(T)| - \left| \int_0^T \{\exp(M\tau)N\}_k w(T-\tau) d\tau \right| \right| \leq \delta.$$

For an input of the form

$$w(t) = \begin{cases} c \cdot \text{sign}(\{\exp(M(T-t))N\}_k) & \text{if } 0 \leq t \leq T \\ 0, & \text{otherwise} \end{cases},$$

we have

$$\begin{aligned} \left| \int_0^T \{\exp(M\tau)N\}_k w(T-\tau) d\tau \right| &= \|w\|_\infty \int_0^T |\{\exp(M\tau)N\}_k| d\tau \\ &= K_k \|w\|_\infty. \end{aligned}$$

Hence

$$|z_k(T)| \geq K_k \|w\|_\infty - \delta.$$

Lemma 1 shows that by choosing δ arbitrarily small, the ultimate bound on the k^{th} state of the stable, linear, time-invariant, single-input system (2.5) will be arbitrarily close to the product of K_k and the infinity norm of the input. Moreover, this bound is actually reached for some bounded input.

REMARK: By corollary 5.2 in [22], z_k is ultimately bounded by

$$\delta + \frac{2[\lambda_{\max}(P)]^2 \|N\|_2}{\lambda_{\min}(P)} \|w\|_\infty, \quad (2.8)$$

where $PM + M^T P = -Q$, for some positive definite matrix Q , where $\lambda_{\max}(P)$, $\lambda_{\min}(P)$ are respectively the largest and smallest eigenvalue of P and $\|N\|_2 = \sqrt{\lambda_{\max}(N^T N)}$. However, choosing Q to minimize the bound (2.8) is not straight forward and Lemma 1 shows that the bound (2.8) can not be smaller than $K_k \|w\|_\infty + \delta$.

We now return to the scaled estimation error governed by (2.4). By Lemma

1 the k^{th} component of the scaled estimation error is ultimately bounded by

$$\begin{aligned} & \|u^{(n)}\|_\infty \int_0^\infty \left| \left\{ \exp\left(\frac{1}{\varepsilon} A \eta \tau\right) B \right\}_k \right| d\tau + \delta \\ & = \varepsilon \|u^{(n)}\|_\infty \int_0^\infty \left| \{ \exp(A \eta \tau) B \}_k \right| d\tau + \delta. \end{aligned}$$

Since $\eta_k = (u^{(k-1)} - \hat{x}_k)/\varepsilon^{n-k}$, the estimation error $(u^{(k-1)} - \hat{x}_k)$ is ultimately bounded by

$$\delta + \varepsilon^{n-k+1} \|u^{(n)}\|_\infty \int_0^\infty \left| \{ \exp(A \eta \tau) B \}_k \right| d\tau, \quad (2.9)$$

for $1 \leq k \leq n-1$.

2.3 The Differentiation Error for Noisy Signals

Let \hat{x} be the state of the observer (2.2) when driven by the noisy measurement $v = u + \mu$, where u is the signal to be differentiated and μ is uniformly bounded measurement noise. By the linearity of the high-gain observer

$$\hat{x} = \xi + \zeta,$$

where

$$\dot{\xi} = \hat{A}\xi + \hat{B}u \quad \text{and} \quad \dot{\zeta} = \hat{A}\zeta + \hat{B}\mu.$$

Without loss of generality, we take $\zeta(0) = 0$. The estimation error can be written as

$$\hat{x}_k - u^{(k-1)} = (\xi_k - u^{(k-1)}) + \zeta_k. \quad (2.10)$$

From equation (2.10) we see that there are two additive components to the differentiation error in the presence of noise. The component $\xi_k - u^{(k-1)}$ is due to the fact that the high-gain observer approximates a differentiator in the limit as the gain approaches infinity, or ε approaches 0, and it is independent of the noise. This component is ultimately bounded by (2.9).

To derive an ultimate bound on ζ_k , consider the change of variables $\hat{\zeta} = D(\varepsilon)\zeta$, where $D(\varepsilon) = \text{diag}[1, \varepsilon, \dots, \varepsilon^{n-1}]$. Since

$$\hat{A} = \frac{1}{\varepsilon}D(\varepsilon)^{-1}A_\eta D(\varepsilon),$$

$\hat{\zeta}$ is governed by the equation

$$\dot{\hat{\zeta}} = \frac{1}{\varepsilon}(A_\eta \hat{\zeta} + \bar{B}\mu),$$

where $\bar{B} = [\alpha_1 \ \alpha_2 \ \dots \ \alpha_{n-1} \ \alpha_n]^T$. Utilizing Lemma 1 we see that $\hat{\zeta}$ is ultimately bounded by

$$\|\mu\|_\infty \int_0^\infty \left| \left\{ \frac{1}{\varepsilon} \exp\left(\frac{1}{\varepsilon} A_\eta \tau\right) \bar{B} \right\}_k \right| d\tau,$$

for $1 \leq k \leq n$. Since $\hat{\zeta}_k = \varepsilon^{k-1} \zeta_k$, ζ_k is ultimately bounded by

$$\frac{1}{\varepsilon^{k-1}} \int_0^\infty |\{\exp(A_\eta \tau) \bar{B}\}_k| d\tau \|\mu\|_\infty, \quad (2.11)$$

for $1 \leq k \leq n$. Set

$$P_k = \int_0^\infty |\{\exp(A_\eta \tau) B\}_k| d\tau,$$

$$Q_k = \int_0^\infty |\{\exp(A_\eta \tau) \bar{B}\}_k| d\tau,$$

for $1 \leq k \leq n$. Relations (2.9), (2.10) and (2.11) allow the ultimate bound on the differentiation error for the k^{th} derivative, where $1 \leq k \leq n - 1$, to take the form

$$\delta + P_{k+1} \|u^{(n)}\|_{\infty} \varepsilon^{n-k} + \frac{Q_{k+1} \|\mu\|_{\infty}}{\varepsilon^k} \equiv b_k(\varepsilon). \quad (2.12)$$

Relation (2.12) outlines the two additive components to the ultimate bound on differentiation error in the presence of measurement noise. One component is directly proportional to a power of ε , whereas the other component is inversely proportional to a power of ε . Although shrinking ε to 0 in the absence of noise improves the differentiation error, the error bound will blow up in the presence of noise since

$$\lim_{\varepsilon \rightarrow 0} b_k(\varepsilon) = \infty, \quad 1 \leq k \leq n - 1.$$

The error bound $b_k(\varepsilon)$, as a function of ε , attains a global minimum for

$$\varepsilon = \varepsilon_k^{opt} = \sqrt[n]{\frac{k}{n-k}} \sqrt[n]{\frac{Q_{k+1} \|\mu\|_{\infty}}{P_{k+1} \|u^{(n)}\|_{\infty}}},$$

since $b'_k(\varepsilon_k^{opt}) = 0$ and $b''_k(\varepsilon) > 0$ for all $\varepsilon > 0$ and $1 \leq k \leq n - 1$. The parameter ε should be of the order $O\left(\sqrt[n]{\frac{\|\mu\|_{\infty}}{\|u^{(n)}\|_{\infty}}}\right)$. Note that the optimal choice for ε depends on the order of the derivative k , meaning that if, for instance, we use a 3^{rd} order high-gain observer, the optimal choice of ε for estimating the first derivative will differ from the optimal choice for estimating the second derivative. However, the order of ε_k^{opt} is the same for all $1 \leq k \leq n - 1$. We show via simulation in the following section that averaging ε_k^{opt} for $1 \leq k \leq n - 1$ does not severely damage the performance of the high-gain observer.

Figure 2.1 depicts the behavior of the bound as a function of ε . It is possible to choose the parameter ε such that a predefined tolerance for the estimation

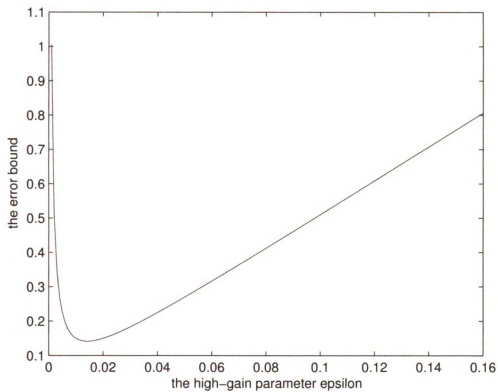


Figure 2.1: The error bound as a function of the high-gain observer parameter ϵ .

error is met. For instance, if the tolerance for the error is 0.3, for any ε between 0.01 and 0.05 the estimation error is guaranteed to be within the tolerance. If $\varepsilon = \varepsilon_k^{opt}$, the error bound takes the form

$$b_k(\varepsilon_k^{opt}) = (Q_{k+1}\|\mu\|_\infty)^{1-\frac{k}{n}}(P_{k+1}\|u^{(n)}\|_\infty)^{k/n} \left(\frac{n}{k} - 1\right)^{k/n} \left(\frac{n}{n-k}\right) + \delta, \quad (2.13)$$

for $1 \leq k \leq n-1$.

The error bound (2.15) depends on the bound on the noise $\|\mu\|_\infty$, the bound on the n^{th} derivative of the signal $\|u^{(n)}\|_\infty$, and through P_k and Q_k , on the eigenvalues of the matrix A_η and the order of the observer n . We will explore this dependence via simulation in the next sections.

The bound (2.12) is not useful unless we can compute P_k and Q_k , for $2 \leq k \leq n$. In the following section, we provide an algorithm to compute P_k and Q_k , for $1 \leq k \leq n$ and illustrate the idea by an example.

2.4 Computation of the Bound

To illustrate how the constants P_k and Q_k , for $1 \leq k \leq n$, could be computed, we start with an example.

Example 1. Suppose we want to design a 3^{rd} order high-gain observer to estimate the first and second derivatives of a bounded signal. Suppose further that we want to place the eigenvalues of the observer at $\lambda_1 = -1, \lambda_2 = -2$, and $\lambda_3 = -3$. The matrices A_η , B and \bar{B} for this choice of eigenvalues are

$$A = \begin{bmatrix} -6 & 1 & 0 \\ -11 & 0 & 1 \\ -6 & 0 & 0 \end{bmatrix}, \quad B = \begin{bmatrix} 0 \\ 0 \\ 1 \end{bmatrix}, \quad \bar{B} = \begin{bmatrix} -6 \\ -11 \\ -6 \end{bmatrix}.$$

The matrices $\exp(A\eta\tau)B$, and $\exp(A\eta\tau)\bar{B}$ are

$$\exp(A\eta\tau)B = \begin{bmatrix} (\frac{1}{2}e^{-3\tau} - e^{-2\tau} + \frac{1}{2}e^{-\tau}) \\ (\frac{3}{2}e^{-3\tau} - 4e^{-2\tau} + \frac{5}{2}e^{-\tau}) \\ (e^{-3\tau} + 3e^{-2\tau} + 3e^{-\tau}) \end{bmatrix}$$

$$\exp(A\eta\tau)\bar{B} = \begin{bmatrix} \frac{27}{2}e^{-3\tau} - 8e^{-2\tau} + \frac{1}{2}e^{-\tau} \\ \frac{81}{2}e^{-3\tau} - 32e^{-2\tau} + \frac{5}{2}e^{-\tau} \\ 27e^{-3\tau} - 24e^{-2\tau} + 3e^{-\tau} \end{bmatrix}.$$

The constants P_k and Q_k are given by

$$\begin{bmatrix} P_1 \\ P_2 \\ P_3 \end{bmatrix} = \begin{bmatrix} \int_0^\infty |(\frac{1}{2}e^{-3\tau} - e^{-2\tau} + \frac{1}{2}e^{-\tau})| d\tau \\ \int_0^\infty |(\frac{3}{2}e^{-3\tau} - 4e^{-2\tau} + \frac{5}{2}e^{-\tau})| d\tau \\ \int_0^\infty |(e^{-3\tau} + 3e^{-2\tau} + 3e^{-\tau})| d\tau \end{bmatrix},$$

$$\begin{bmatrix} Q_1 \\ Q_2 \\ Q_3 \end{bmatrix} = \begin{bmatrix} \int_0^\infty |\frac{27}{2}e^{-3\tau} - 8e^{-2\tau} + \frac{1}{2}e^{-\tau}| d\tau \\ \int_0^\infty |\frac{81}{2}e^{-3\tau} - 32e^{-2\tau} + \frac{5}{2}e^{-\tau}| d\tau \\ \int_0^\infty |27e^{-3\tau} - 24e^{-2\tau} + 3e^{-\tau}| d\tau \end{bmatrix}.$$

We show in detail how to compute

$$Q_2 = \int_0^\infty |(\frac{81}{2}e^{-3\tau} - 32e^{-2\tau} + \frac{5}{2}e^{-\tau})| d\tau.$$

Denote $g(t) = (\frac{81}{2}e^{-3t} - 32e^{-2t} + \frac{5}{2}e^{-t})$. We want to compute

$$\int_0^\infty |g(t)| dt.$$

Figure 2.2 displays the graph of $g(t)$. Recall that the definite integral is the numerical value of the area between the graph of the function and the abscissa.

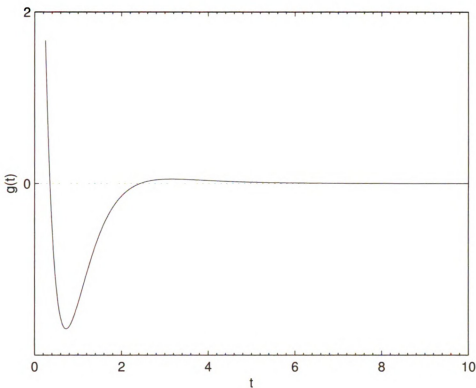


Figure 2.2: The function $g(t)$.

The function $g(t)$ has zeros at $t_1 = 0.3535$ and $t_2 = 2.4315$. We evaluate

$$\int_0^{\infty} |g(t)| dt = \int_0^{t_1=0.3535} g(t) dt + \left| \int_{t_1=0.3535}^{t_2=2.4315} g(t) dt \right| + \int_{t_2=2.4315}^{\infty} g(t) dt.$$

In other words, to evaluate the integral of the absolute value of a function, we add up the absolute values of the integrals of the function between its zeros. Symbolic software like MATLAB and Mathematica has the capacity to compute P_k and Q_k , for $1 \leq k \leq n$, for a given linear system. We provide as an Appendix to this thesis a MATLAB script that computes the constants P_k and Q_k , for $1 \leq k \leq n$, from the eigenvalues of the matrix $A\eta$. Application of the script to

the current example yields

$$\begin{bmatrix} P_1 \\ P_2 \\ P_3 \end{bmatrix} = \begin{bmatrix} 0.1667 \\ 1 \\ 1.8333 \end{bmatrix}, \quad \begin{bmatrix} Q_1 \\ Q_2 \\ Q_3 \end{bmatrix} = \begin{bmatrix} 1.4116 \\ 3.1297 \\ 1.8292 \end{bmatrix}.$$

We now summarize the algorithm. To compute P_k and Q_k , where $1 \leq k \leq n$,

- Compute the matrix $\exp(A_\eta t)$
- Compute the k^{th} entry $F_k(t)$ of the n-dimensional vector function $F(t) = \exp(A_\eta t)B$
- Compute the k^{th} entry $G_k(t)$ of the n-dimensional vector function $G(t) = \exp(A_\eta t)\bar{B}$
- Find the zeros of $F_k(t)$
- Find the zeros of $G_k(t)$
- To compute P_k , integrate $F_k(t)$ between its zeros and add the absolute values of the obtained integrals
- To compute Q_k , integrate $G_k(t)$ between its zeros and add the absolute values of the obtained integrals

2.5 Conservatism of the Bound

The bound given by (2.12) is conservative in the sense that it does not take into account the low-pass filtering characteristics of the high-gain observer. To illustrate this point, consider the transfer function of a 2^{nd} order high-gain observer that

estimates the first derivative of the input:

$$T(s) = \frac{\alpha_2 s}{\varepsilon^2 s^2 + \varepsilon \alpha_1 s + \alpha_2}. \quad (2.14)$$

For a sinusoidal noise μ of frequency ω ,

$$\|\zeta_k\|_\infty \leq |T(j\omega)| \|\mu\|_\infty,$$

whereas

$$|T(j\omega)| = \frac{\alpha_2 \omega}{\sqrt{(\alpha_2 - \omega^2 \varepsilon^2)^2 + (\alpha_1 \omega \varepsilon)^2}}.$$

The resonance frequency for the second-order system (2.14) that maximizes $|T(j\omega)|$

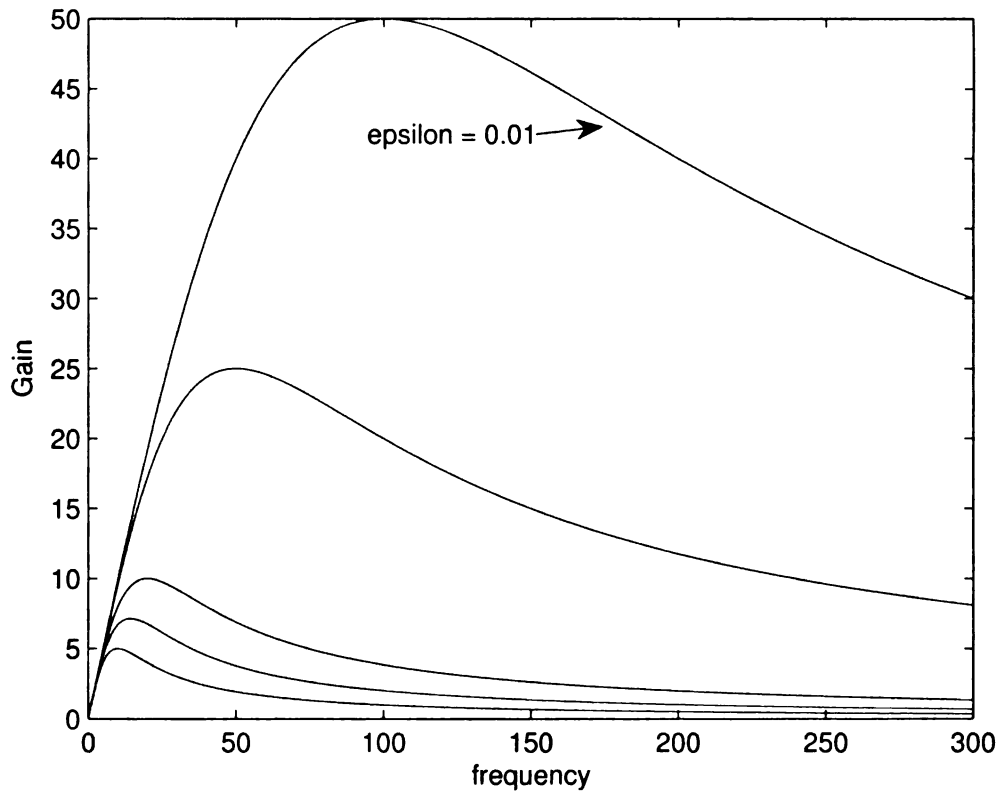


Figure 2.3: The gain of the high-gain observer as a function of frequency.

is of the order $O\left(\frac{1}{\varepsilon}\right)$. Although the resonance frequency might achieve the bound $b(\varepsilon)$ in (2.12), the low-pass feature of the high-gain observer will diminish the high-frequency noise since $|T(j\omega)| \rightarrow 0$ as $\omega \rightarrow \infty$; hence, the high-frequency components of the noise will be attenuated due to the low-pass filtering characteristics of the high-gain observer. Figure 2.3 shows the plots of $|T(j\omega)|$ as a function of the frequency ω for several values of ε . Note that the gain increases as ε decreases; however, it is always a bounded function and it rolls off for high frequencies.

2.6 Computer Simulation

2.6.1 The Effect of the Eigenvalues and the Order of the Observer on the Error Bound

Recall from (2.12) that the value of ε that minimizes the error bound $b_k(\varepsilon)$ where the k^{th} derivative is estimated with an n^{th} order high-gain observer is given by

$$\varepsilon = \varepsilon_k^{opt} = \sqrt[n]{\frac{k}{n-k}} \sqrt[n]{\frac{Q_{k+1}\|\mu\|_\infty}{P_{k+1}\|u^{(n)}\|_\infty}},$$

whereas

$$b_k(\varepsilon_k^{opt}) = (Q_{k+1}\|\mu\|_\infty)^{1-\frac{k}{n}} (P_{k+1}\|u^{(n)}\|_\infty)^{k/n} \left(\frac{n}{k} - 1\right)^{k/n} \left(\frac{n}{n-k}\right). \quad (2.15)$$

The error bound (2.15) depends on the magnitude of the noise $\|\mu\|_\infty$, the bound on the n^{th} derivative of the signal $\|u^{(n)}\|_\infty$, and through P_k and Q_k , the

eigenvalues of the matrix A_η and the order of the observer n . In (2.15) only

$$Q_{k+1}^{(1-\frac{k}{n})} P_{k+1}^{k/n} \quad (2.16)$$

depends on the eigenvalues of the matrix A_η . To investigate the dependence of (2.16) on the eigenvalues of the matrix A_η , we computed (2.16) for different sets of eigenvalues. These results are summarized in Tables 2.1, 2.2, 2.3 and 2.4. Since the eigenvalues of the high-gain observer are equal to the eigenvalues of A_η rescaled by $\frac{1}{\varepsilon}$, it is not surprising that the value of (2.16) does not change if all eigenvalues of A_η are rescaled by the same constant. In other words, rescaling the eigenvalues of A_η will result in a rescaled ε_k^{opt} , but the bound $b_k(\varepsilon_k^{opt})$ will not change.

Table 2.1: The constant $\sqrt{Q_2 P_2}$ for $k = 1$ and $n = 2$

Eigenvalues:	Eigenvalues:	Eigenvalues:	Eigenvalues:	Eigenvalues:
-1, -1	-1, -3	-1, -5	-1, -10	$e^{\pm \frac{j3\pi}{4}}$
1.2131	1.2408	1.2669	1.3051	1.1356

Table 2.2: The expression $Q_{k+1}^{(1-\frac{k}{n})} P_{k+1}^{k/n}$ for $1 \leq k \leq 2$ and $n = 3$

Derivative	Eigenvalues:	Eigenvalues:	Eigenvalues:	Eigenvalues:
	-1, -1, -1	-1, -3, -5	-1, -5, -10	$-1, e^{\pm \frac{j2\pi}{3}}$
1 st : $P_2^{\frac{1}{3}} Q_2^{\frac{2}{3}}$	2.0950	2.2135	2.3937	1.7607
2 nd : $P_3^{\frac{2}{3}} Q_3^{\frac{1}{3}}$	1.7737	1.9150	2.0928	1.3608

When the eigenvalues are real, the error bound is smallest for equal, multiple eigenvalues, and it increases as the distance between eigenvalues increases.

Table 2.3: The expression $Q_{k+1}^{(1-\frac{k}{n})} P_{k+1}^{k/n}$ for $1 \leq k \leq 3$ and $n = 4$

Derivative	Eigenvalues:	Eigenvalues:	Eigenvalues:	Eigenvalues:
	-1, -1, -1,	-1, -5, -10,	-1, -1,	$e^{\pm j\frac{2\pi}{3}}, e^{\pm j\frac{5\pi}{6}}$
	-1	-15	$e^{\pm j\frac{3\pi}{4}}$	
$1^{st} : P_2^{\frac{1}{4}} Q_2^{\frac{3}{4}}$	3.2164	3.8403	2.6351	2.4524
$2^{nd} : P_3^{\frac{2}{3}} Q_3^{\frac{1}{3}}$	3.6065	5.0592	2.6456	2.3237
$3^{rd} : P_4^{\frac{3}{4}} Q_4^{\frac{1}{4}}$	2.4465	3.5602	2.7560	2.3306

The error bound is smaller for complex eigenvalues distributed on a semi-circle of radius one in a butterworth structure than for real, multiple eigenvalues. However, it is argued in [9] that although the steady-state error is smaller for complex eigenvalues, the transient response is oscillatory and the transient time is longer than for multiple, real eigenvalues. To investigate this phenomenon, we simulated real time differentiation with a 2^{nd} , 3^{rd} and 4^{th} order high-gain observer for both choices of eigenvalues: multiple real and complex eigenvalues distributed on a semi-circle in a butterworth structure. We differentiated noisy and noise-free sinusoids.

We simulated high-gain observers (2.2) for $n = 2$, $n = 3$ and $n = 4$. The signal we differentiated is $u(t) = \sin(t)$, where t is time. In the absence of noise, we set $\varepsilon = 0.01$. For the 2^{nd} order observer; for A_η with eigenvalues $\lambda_{1/2} = e^{\pm j\frac{3\pi}{4}}$, the coefficients of the observer are $\alpha_1 = 1.4142$ and $\alpha_2 = 1$. For A_η with multiple real eigenvalues placed at -1, we have $\alpha_1 = 2$ and $\alpha_2 = 1$. Figure 2.4 shows the estimation error, where the first derivative is estimated with a 2^{nd} order high-gain observer. The amplitude of the steady-state error for complex eigenvalues is 0.014 and 0.02 for real eigenvalues.

Table 2.4: The expression $Q_{k+1}^{(1-\frac{k}{n})} P_{k+1}^{k/n}$ for $1 \leq k \leq 4$ and $n = 5$

Derivative	Eigenvalues: -1, -1, -1, -1, -1	Eigenvalues: -1, -2, -3, -4, -5	Eigenvalues: -1, -3, -5, -7, -9	Eigenvalues: -1, -5, -10, -15, -20
1 st : $P_2^5 Q_2^5$	4.5223	4.7229	4.979	5.5275
2 nd : $P_3^5 Q_3^5$	6.5034	7.2341	8.0703	9.9357
3 rd : $P_4^5 Q_4^5$	5.7919	6.5768	7.5188	9.7568
4 th : $P_5^5 Q_5^5$	3.1808	3.4989	3.8921	4.8245

For the 3rd order observer; for A_η with eigenvalues $\lambda_{1/2} = e^{\pm \frac{j3\pi}{4}}$, $\lambda_3 = -1$, we have $\alpha_1 = \alpha_2 = 2.4142$ and $\alpha_3 = 1$, whereas $\alpha_1 = \alpha_2 = 3$ and $\alpha_3 = 1$ if A_η has multiple real eigenvalues placed at -1. Figure 2.5 shows the estimation error, where the 1st and 2nd derivatives are estimated with a 3rd order high-gain observer. For the first derivative, the amplitude of the steady-state error for complex eigenvalues is 0.00024, for real eigenvalues 0.000299. For the second derivative, the amplitude of the steady-state error for complex eigenvalues is 0.024, for real eigenvalues 0.03.

For the 4th order observer; for A_η with eigenvalues $\lambda_{1/2} = e^{\pm \frac{j2\pi}{3}}$, $\lambda_{3/4} = e^{\pm \frac{j5\pi}{6}}$, the coefficients of the observer are $\alpha_1 = \alpha_3 = 2.7321$, $\alpha_2 = 3.7321$, and $\alpha_4 = 1$. For A_η with multiple real eigenvalues placed at -1, the coefficients are $\alpha_1 = \alpha_3 = 4$, $\alpha_2 = 6$, and $\alpha_4 = 1$. Figure 2.6 shows the estimation error, where the 1st, 2nd and 3rd derivatives are estimated with a 4th order high-gain observer. For the first derivative, the amplitude of the steady-state error for complex eigenvalues is 0.000002, for real eigenvalues 0.000004. For the second derivative, the amplitude of the steady-state error for complex eigenvalues is

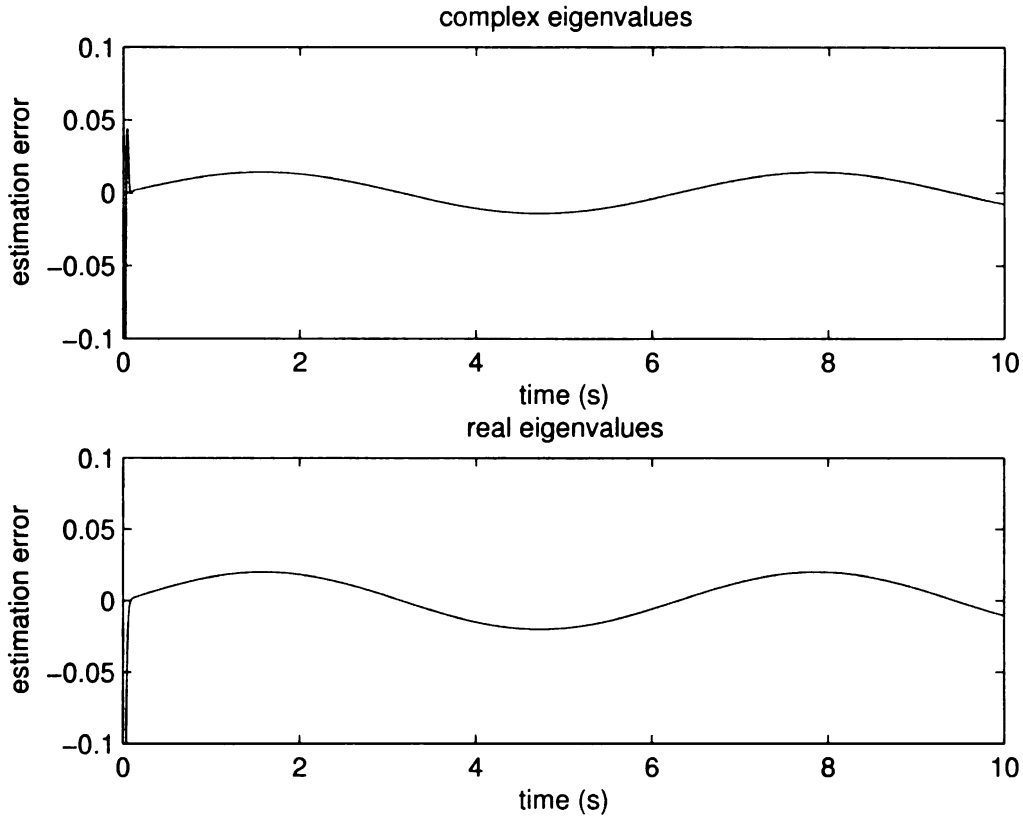


Figure 2.4: The estimation error as a function of time. The first derivative of a sinusoidal signal is estimated with a second order high-gain observer with $\varepsilon = 0.01$.

0.00037, for real eigenvalues 0.0006. For the third derivative, the amplitude of the steady-state error for complex eigenvalues is 0.027, for real eigenvalues 0.04. Although the steady-state error might be smaller with complex eigenvalues, the transient response is more oscillatory and the transient time is longer than with multiple, real eigenvalues.

In the absence of noise, the estimation error is bounded by

$$\varepsilon^{n-k+1} \|u^{(n)}\|_{\infty} P_k, \quad 1 \leq k \leq n, \quad (2.17)$$

where k is the estimated derivative and n is the order of the observer. In the absence of noise, reducing ε improves the estimation error. For $\varepsilon < 1$, ε^{n-k+1}

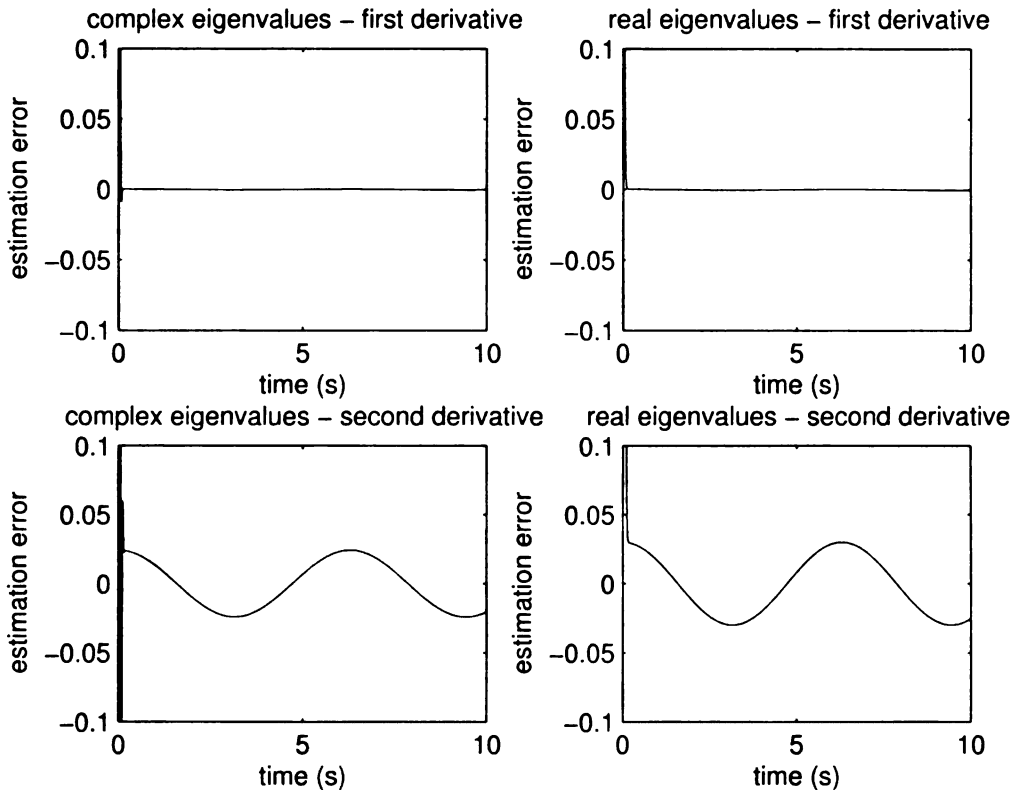


Figure 2.5: The estimation error as a function of time. The derivatives of a sinusoidal signal are estimated with a third order high-gain observer with $\varepsilon = 0.01$.

is a decreasing function of the order of the observer n . On the other hand, we observed from simulation that for a fixed derivative k , P_k is an increasing function of the order of the observer n . Whether the bound (2.17) increases or decreases as a function of the order n , depends on the choice of ε , the order of the estimated derivative k , and the differentiated signal through $\|u^{(n)}\|_\infty$. Figures 2.4, 2.5 and 2.6 indicate that for $\varepsilon = 0.01$ and $u(t) = \sin(t)$, the estimate of the first derivative with a 4th order observer is better than the one with a 3rd order observer, whereas the estimate with a 3rd order observer is better than the estimate with a 2nd order observer. Also, Figures 2.5 and 2.6 indicate that for $\varepsilon = 0.01$ and $u(t) = \sin(t)$, the estimate of the second derivative with a 4th order observer is better than the estimate of the second derivative with a 3rd order observer.

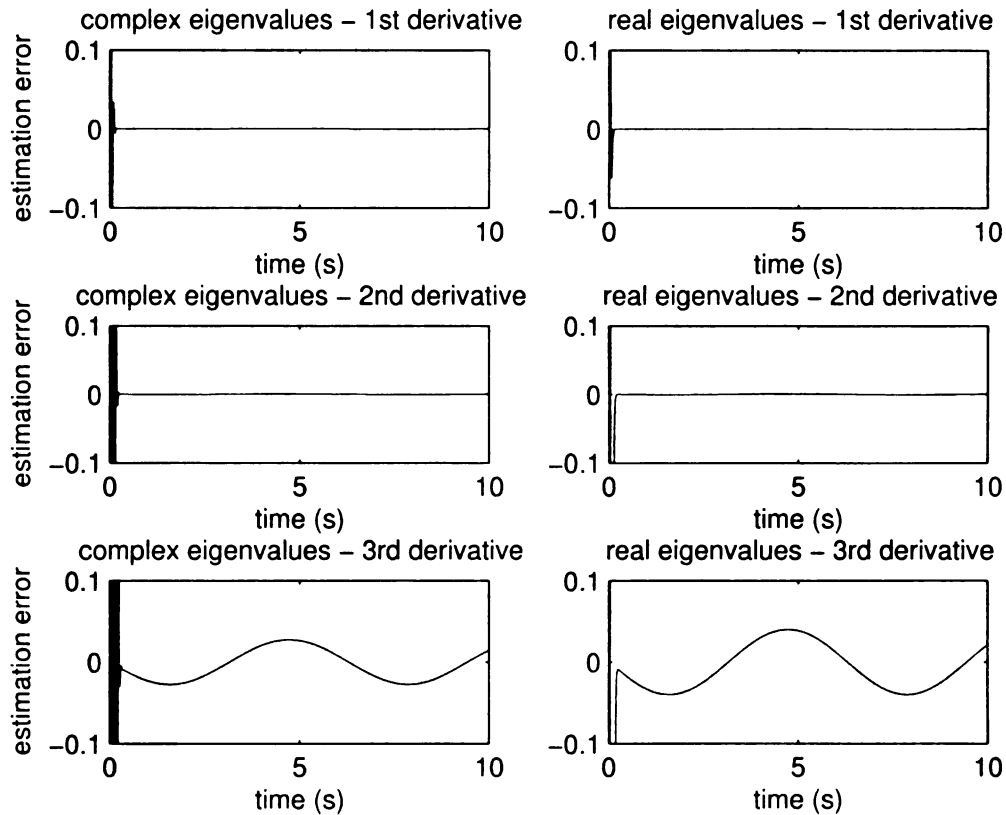


Figure 2.6: The estimation error as a function of time. The first derivative of a sinusoidal signal is estimated with a fourth order high-gain observer with $\varepsilon = 0.01$.

To investigate the effect of the eigenvalues of A_η on the estimation error in the presence of measurement noise, we differentiated the signal $u_{noisy}(t) = \sin(t) + \mu(t)$, where $\mu(t)$ is noise obtained from SIMULINK Band-Limited White Noise generator. The noise power is 10^{-8} , sampling time 0.001 seconds. Figure 2.7 displays the noise in time and frequency domain.

We chose the parameter ε as $\frac{1}{n-1} \sum_{k=1}^{n-1} \varepsilon_k^{opt}$, where $n = 2, 3$ or 4 . To justify this choice we show in Figure 2.8 the error bound $b_k(\varepsilon)$ as a function of ε , given by relation (2.12), for a 4^{th} order high-gain observer with multiple real eigenvalues. If $u(t) = \sin(t)$, then $\|u^{(4)}\|_\infty = 1$. We took $\|\mu\|_\infty = 0.012$. The value of ε that minimizes the error bound for the first derivative $b_1(\varepsilon)$ is $\varepsilon_1^{opt} = 0.2339$. The value of ε that minimizes the error bound for the second

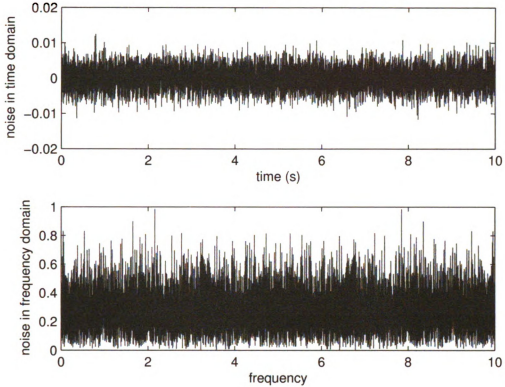


Figure 2.7: The noise $\mu(t)$ in time and frequency domain.

derivative $b_2(\varepsilon)$ is $\varepsilon_2^{opt} = 0.2566$. The value of ε that minimizes the error bound for the third derivative $b_3(\varepsilon)$ is $\varepsilon_3^{opt} = 0.2664$. For the 4th high-gain observer with real multiple eigenvalues we set $\varepsilon = (0.2339 + 0.2566 + 0.2664)/3 = 0.2523$. Note that this choice of ε does not significantly increase the error bound for the derivatives.

For the 2nd order observer with multiple real eigenvalues, $\varepsilon_1^{opt} = 0.0664$. For the 2nd order observer with complex eigenvalues, $\varepsilon_1^{opt} = 0.087963$. Figure 2.9 displays the estimation error for the first derivative with a 2nd order high-gain observer.

For the 3rd order observer with multiple real eigenvalues, we set $\varepsilon = (\varepsilon_1^{opt} + \varepsilon_2^{opt})/2 = 0.1612$. For the 3rd order observer with complex eigenvalues,

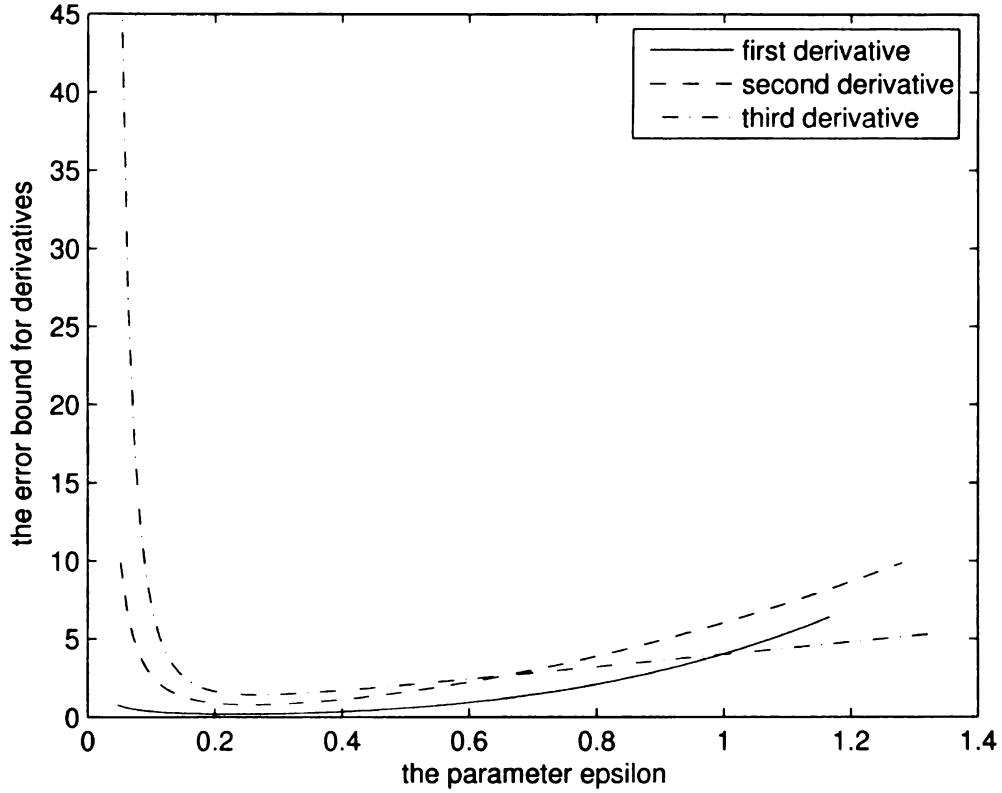


Figure 2.8: The error bound for the derivatives as a function of ε for a 4th order high-gain observer with multiple real eigenvalues.

we set $\varepsilon = (\varepsilon_1^{opt} + \varepsilon_2^{opt})/2 = 0.16739$. Figure 2.10 displays the estimation error for the first and second derivatives with a 3rd order high-gain observer.

For the 4th order observer with multiple real eigenvalues, we set $\varepsilon = (\varepsilon_1^{opt} + \varepsilon_2^{opt} + \varepsilon_3^{opt})/3 = 0.2523$. For the 4th order observer with complex eigenvalues, we set $\varepsilon = (\varepsilon_1^{opt} + \varepsilon_2^{opt} + \varepsilon_3^{opt})/3 = 0.26093$. Figure 2.11 displays the estimation error for the first, second and third derivatives with a 4th order high-gain observer.

Recall that $b_k(\varepsilon_k^{opt})$, given by (2.15) for a fixed $1 \leq k \leq n-1$, depends on the order of the observer n . We observed that $Q_{k+1}^{1-\frac{k}{n}} P_{k+1}^{k/n} \left(\frac{n}{k} - 1\right)^{k/n} \left(\frac{n}{n-k}\right)$ is an increasing function of the order of the observer n for a fixed $1 \leq k \leq n-1$. Hence, whether the error bound $b_k(\varepsilon_k^{opt})$ for a fixed $1 \leq k \leq n-1$, is an

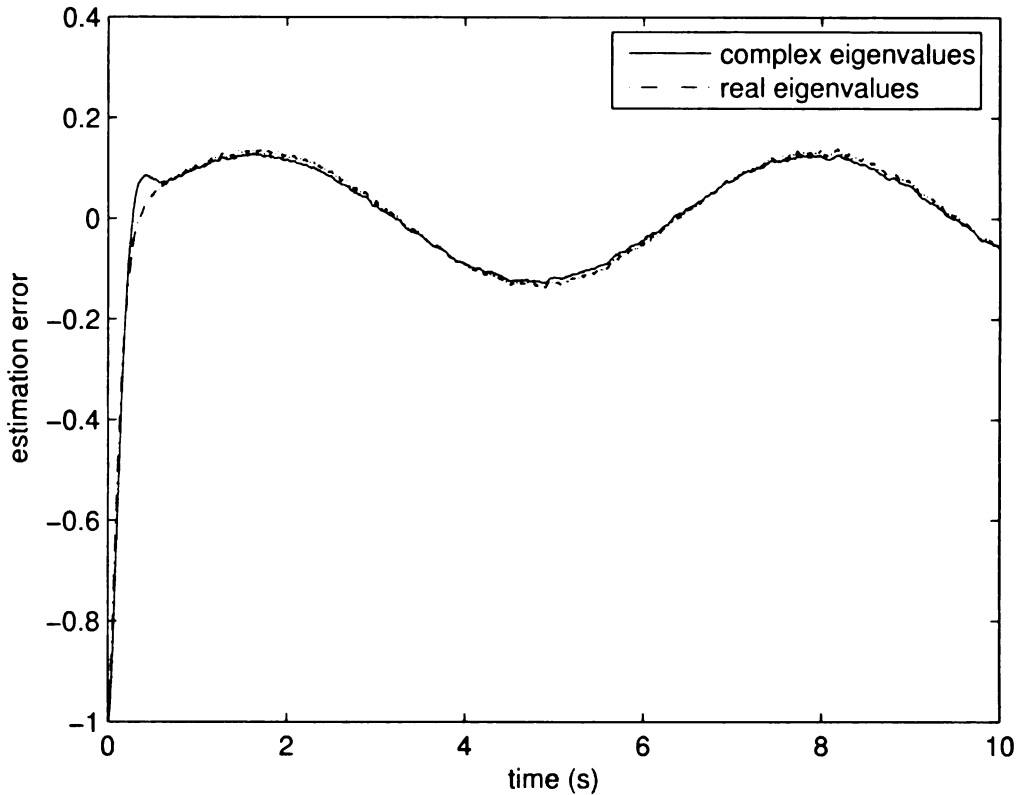


Figure 2.9: The estimation error as a function of time. The first derivative of a noisy sinusoidal signal is estimated with a 2^{nd} order high-gain observer. The magnitude of the noise is $\|\mu\|_\infty = 0.012$, $\|u''\|_\infty = 1$, and $\varepsilon = \varepsilon_1^{opt}$.

increasing or a decreasing function of the order of the observer n , depends on the ratio $\|u^{(n)}\|_\infty / \|\mu\|_\infty$. Clearly, if $\|u^{(n)}\|_\infty / \|\mu\|_\infty \leq 1$, the error bound is an increasing function of the order n and it is best to estimate the k^{th} derivative with an observer of order $k + 1$. But if $\|u^{(n)}\|_\infty / \|\mu\|_\infty > 1$, it might be better to estimate the k^{th} derivative with an observer of order higher than $k + 1$.

In our simulation, for $u(t) = \sin(t)$ and $\|\mu\|_\infty = 0.012$, the estimate of the first derivative with a 4^{th} order observer is better than the estimate with a 3^{rd} order observer, which is better than the estimate with a 2^{nd} order observer. Also, the estimate of the second derivative with a 4^{th} order observer is better than the estimate of the second derivative with a 3^{rd} order observer. For the

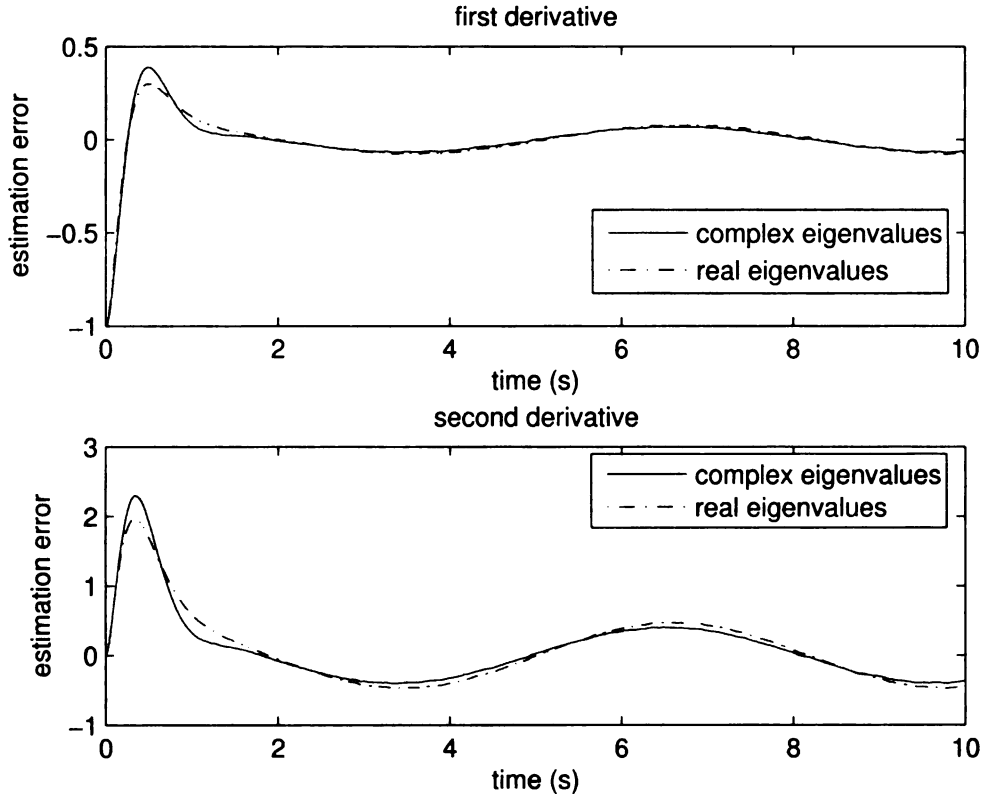


Figure 2.10: The estimation error as a function of time. The derivatives of a noisy sinusoidal signal are estimated with a 3^{rd} order high-gain observer. The magnitude of the noise is $\|\mu\|_\infty = 0.012$, $\|u^{(3)}\|_\infty = 1$, and $\varepsilon = (\varepsilon_1^{opt} + \varepsilon_2^{opt})/2$.

convenience of practicing engineers, we provide as an Appendix to this thesis a table of the constants P_k and Q_k for $2 \leq k \leq n$, $2 \leq n \leq 10$ for multiple real eigenvalues.

2.6.2 Comparison Between the Actual Estimation Error and the Error Bound

To investigate how the estimation error relates to the error bound (2.12), we simulated differentiation in the presence of measurement noise for three different sig-

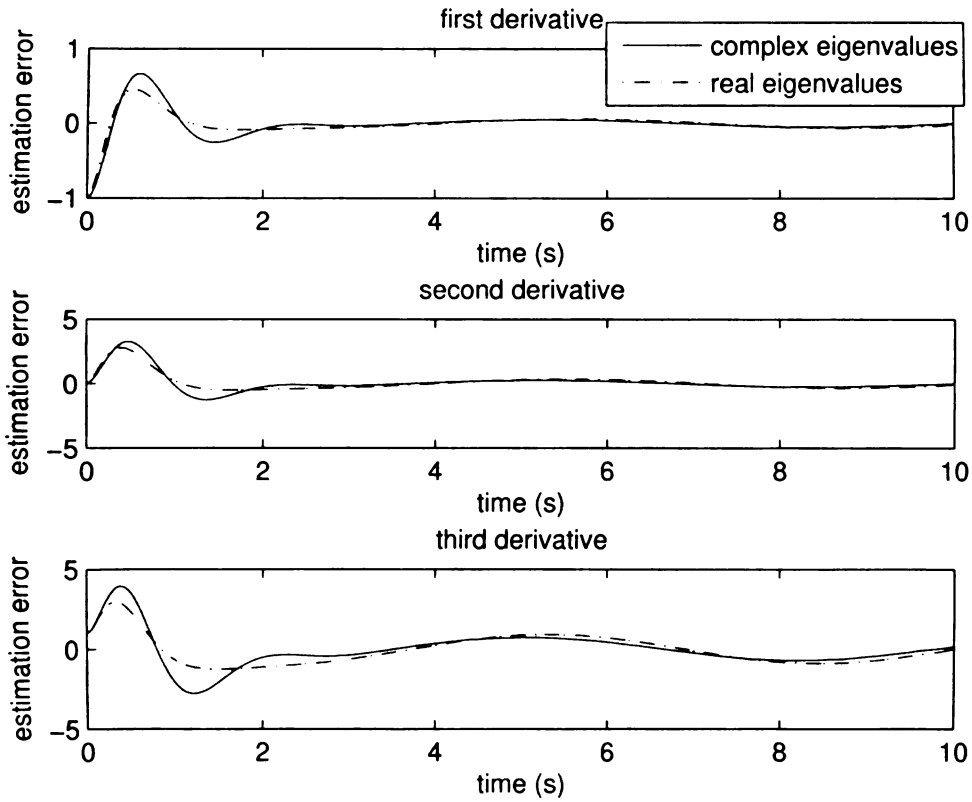


Figure 2.11: The estimation error as a function of time. The derivatives of a noisy sinusoidal signal are estimated with a 4^{th} order high-gain observer. The magnitude of the noise is $\|\mu\|_\infty = 0.012$, $\|u^{(4)}\|_\infty = 1$, and $\varepsilon = (\varepsilon_1^{opt} + \varepsilon_2^{opt} + \varepsilon_3^{opt})/3$.

nals. For a noisy signal³ $u_{noisy}(t) = u(t) + \mu(t)$, we varied the parameter ε and computed the steady-state error as $\max_{t \geq T} |u^{(k)}(t) - \hat{x}_{k+1}|$, where \hat{x}_k is the k^{th} state of the high-gain observer with input $u_{noisy}(t)$, t is time, and $T > 0$ is transient time. We used a 3^{rd} order high-gain observer with multiple real eigenvalues in the simulation.

³The noise $\mu(t)$ is noise obtained from SIMULINK Band-Limited White Noise generator. The noise power is 10^{-8} , sampling time 0.0001 seconds. Figure 2.7 displays the noise in time and frequency domain.

For $u(t)$ being the state $x_1(t)$ of the 3^{rd} order nonlinear system⁴

$$\begin{bmatrix} \dot{x}_1 \\ \dot{x}_2 \\ \dot{x}_3 \end{bmatrix} = \begin{bmatrix} 0 & 1 & 0 \\ 0 & 0 & 1 \\ 0 & 0 & 0 \end{bmatrix} \begin{bmatrix} x_1 \\ x_2 \\ x_3 \end{bmatrix} + \begin{bmatrix} 0 \\ 0 \\ 1 \end{bmatrix} b(x_1, x_2, x_3),$$

$$u = x_1,$$

$$b(x_1, x_2, x_3) = \alpha(x_1, x_2, x_3)g_s(x_1, x_2, x_3) + (1 - \alpha(x_1, x_2, x_3))g_u(x_1, x_2, x_3),$$

$$\alpha(x_1, x_2, x_3) = 2 \frac{x_1^2 + x_2^2 + x_3^2}{1 + x_1^2 + x_2^2 + x_3^2},$$

$$g_s(x_1, x_2, x_3) = -54x_1 - 36x_2 - 9x_3,$$

$$g_u(x_1, x_2, x_3) = 54x_1 - 36x_2 + 9x_3,$$
(2.18)

the actual estimation error compared to the error bound for the derivatives is depicted in Figure 2.12.

For

$$u = y - [10\sin(0.05x) + 5],$$
(2.19)

where x and y are the states of the system⁵

$$\begin{aligned} \dot{x} &= \nu \cos\varphi, \\ \dot{\varphi} &= \frac{\nu}{5} \tan\theta, \\ \dot{\theta} &= c, \\ \dot{y} &= \nu \sin\varphi, \\ c &= -20 \operatorname{sign}\{u^{(3)} + 3(\ddot{u}^6 + \dot{u}^4 + |u|^3)^{1/12} \times \operatorname{sign}[\ddot{u} + (\dot{u}^4 + |u|^3)^{1/6} \\ &\quad \times \operatorname{sign}(\dot{u} + 0.5|u|^{3/4} \operatorname{sign}(u))]\}, \end{aligned}$$

the actual estimation error compared to the error bound for the derivatives is depicted in Figure 3.3. For $u(t) = \sin(t)$, the actual estimation error compared

⁴System (3.4) was used in [10] and [9] to test a numerical differentiator.

⁵The signal (2.19) is taken from [25].

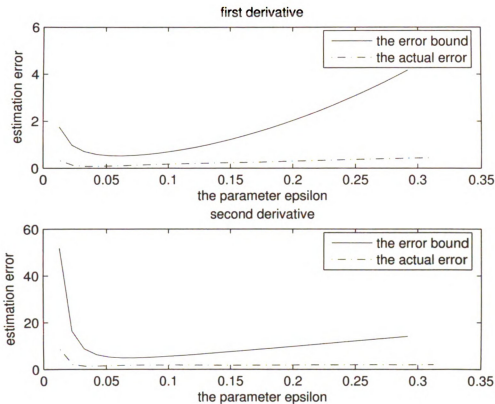


Figure 2.12: Actual error compared to the error bound (2.12) for estimating the first and second derivative of u as described by (3.4) with a 3^{rd} order high-gain observer.

to the error bound for the derivatives is depicted in Figure 3.1. Note that for all signals used in this simulation; that is $u(t)$ given by (3.4), $u(t)$ given by (2.19) and $u(t) = \sin(t)$, the value of ε that yields the smallest error differs from ε_k^{opt} , which minimizes the error bound $b_k(\varepsilon)$ (2.12). Relation (2.12) means that for all signals with $\|u^{(n)}\|_\infty \leq \Delta$, the error is guaranteed to be less than

$$P_{k+1}\Delta\varepsilon^{n-k} + \frac{Q_{k+1}\|\mu\|_\infty}{\varepsilon^k}.$$

Choosing $\varepsilon = \varepsilon_k^{opt}$ to minimize the error bound $b_k(\varepsilon)$, guarantees that the estimation error will be less than $b_k(\varepsilon_k^{opt})$, which is not violated in simulation. It

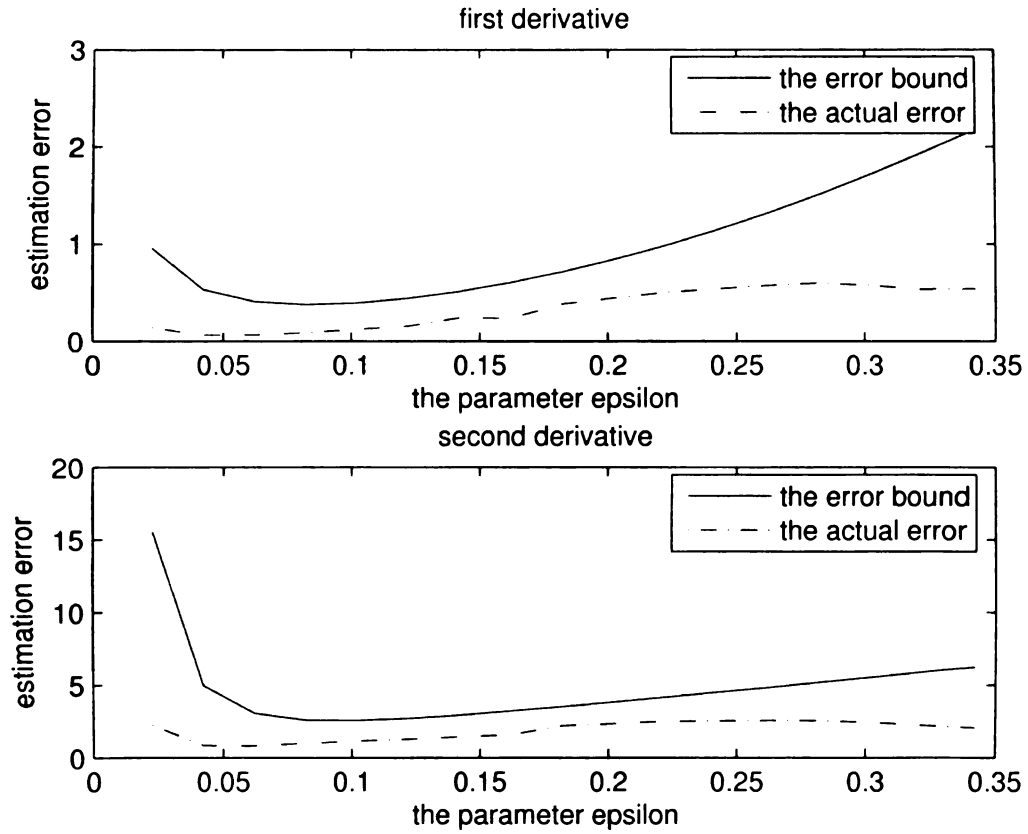


Figure 2.13: Actual error compared to the error bound (2.12) for estimating the first and second derivative of u given by (2.19) with a 3^{rd} order high-gain observer.

is interesting to observe that the "best" ε for some signals with $\|u^{(n)}\|_{\infty} \leq \Delta$, could be different than ε_k^{opt} . However, the analytic choice of ε is consistent with the actual error.

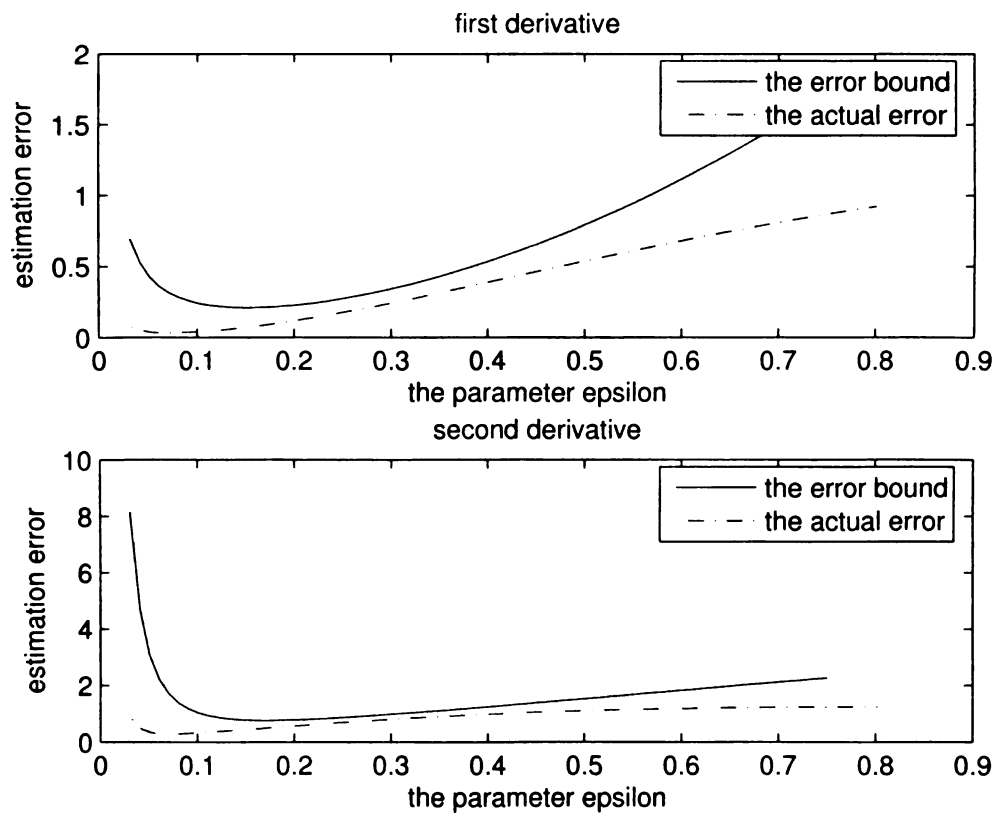


Figure 2.14: Actual error compared to the error bound (2.12) for estimating the first and second derivative of $u(t) = \sin(t)$ with a 3^{rd} order high-gain observer.

Chapter 3

A Comparison Between High-Gain Observers and Exact Robust Sliding-Mode Differentiators

In this chapter we review arbitrary order robust, exact sliding-mode differentiators developed by A. Levant in [24] and [25], compare their features to the features of high-gain observers and compare the performance of the two observers via extensive simulation in the presence of measurement noise.

3.1 Robust Exact Differentiation via Sliding Mode Technique

In [24] and [25] A. Levant developed differentiators that are exact in the absence of noise after some transient time that could be made arbitrarily small, and provide

for an error bound of the order $O(\|\mu\|_\infty^{1-k/n} \|u^{(n)}\|_\infty^{k/n})$, in the presence of noise, if μ is uniformly bounded noise, where the k^{th} derivative is estimated and $n > k$, provided that the n^{th} derivative of the differentiated signal u is bounded. We state the theorems about robust exact differentiator as presented by A. Levant in [24] and [25]. See [24] and [25] for proofs of the stated theorems.

Let the input signal $u_{noisy}(t) = u(t) + \mu(t)$, be a measurable locally bounded function defined on $[0, \infty)$, $u(t)$ is the base signal that has a derivative with Lipschitz's constant¹ $L > 0$ and $\mu(t)$ is noise. The differentiation problem is formulated as a control problem to keep the constraint $s = u - x = 0$. For 2-sliding we have $\dot{s} = \dot{x} - \dot{u} = 0$, and hence $\dot{u} = \dot{x}$. Toward that end, consider the auxiliary equation

$$\dot{x} = y. \quad (3.1)$$

Applying a modified 2-sliding algorithm (See [26]) to keep $x - u(t) = 0$, we obtain

$$\begin{aligned} y &= y_1 - \lambda |x - u_{noisy}(t)|^{1/2} \text{sign}(x - u_{noisy}(t)), \\ y_1 &= -\alpha \text{sign}(x - u_{noisy}(t)), \end{aligned} \quad (3.2)$$

To ensure 2-sliding on $s = x - u = 0$, define $\Phi(\alpha, \lambda, L) = |\Psi(t_*)|$, where $(\Sigma(t), \Psi(t))$ is the solution of

$$\begin{aligned} \dot{\Sigma} &= -|\Sigma|^{1/2} + \Psi, \\ \dot{\Psi} &= \begin{cases} -\frac{1}{\lambda^2}(\alpha - L), & -|\Sigma|^{1/2} + \Psi > 0 \\ -\frac{1}{\lambda^2}(\alpha + L), & -|\Sigma|^{1/2} + \Psi \leq 0 \end{cases}, \\ \Sigma(0) &= 0, \quad \Psi(0) = 1, \quad \alpha > L, \quad \lambda > 0 \text{ and} \\ t_* &= \inf \{t \mid t > 0, \Sigma(t) = 0, \Psi(t) < 0\}. \end{aligned} \quad (3.3)$$

¹If the input $u(t)$ is twice differentiable with bounded second derivative, the Lipschitz's constant of the first derivative is equal to $\|u''\|_\infty$.

Choose $\alpha > L, \lambda > 0$ and $\Phi(\alpha, \lambda, L) < 1$. The output of the system (3.1), (3.2) is $y(t) = \dot{x}(t) = u'(t)$, whereas the solutions of (3.1), (3.2) are understood in the Filippov sense [17]. In practice $\Phi(\alpha, \lambda, L)$ is to be calculated via computer simulation.

Theorem 1 *Let $\alpha > L, \lambda > 0$ such that $\Phi(\alpha, \lambda, L) < 1$. Then, with $\mu(t) \equiv 0$, provided $u(t)$ has a derivative with Lipschitz's constant L , the equality $y(t) = u'(t)$ is fulfilled identically after a finite time transient process.*

Theorem 1 means that after a finite transient time, the output of the differentiator (3.1) and (3.2) is the exact derivative of the input in the absence of noise, provided that (3.3) holds. It could be inferred from the proof of Theorem 1 [24] that smaller $\Phi(\alpha, \lambda, L)$, yields faster convergence of $y(t)$ to $u'(t)$. Also, for fixed α , increasing λ decreases Φ . A sufficient condition for convergence, resulting from a crude estimation is

$$\alpha > L, \quad \lambda^2 \geq 4L \frac{\alpha + L}{\alpha - L}.$$

The substitutions $\alpha = k_1 L, \lambda = k_2 \sqrt{L}$, for $k_1 > 1, k_2 > 0$ in (3.3) eliminate L from the equations for ϕ enabling ϕ to be computed regardless of the Lipschitz constant L . Some triplets of λ, α , and ϕ are: $\lambda = \sqrt{L}, \alpha = 1.1L, \Phi = 0.9888$ and $\lambda = 0.5\sqrt{L}, \alpha = 4L, \Phi = 0.736$.

Theorem 2 *Let $\alpha > L, \lambda > 0$ such that $\Phi(\alpha, \lambda, L) < 1$. Then, for $\mu(t)$ with $\|\mu\|_\infty < \infty$, provided $u(t)$ has a derivative with Lipschitz's constant L , the inequality $|c(t) - u'(t)| < \lambda b \sqrt{\|\mu\|_\infty}$ holds after a finite time transient process, for some $b(\frac{\alpha-L}{\lambda^2}, \frac{\alpha+L}{\lambda^2}) > 0$.*

If $\alpha = k_1 L, \lambda = k_2 \sqrt{L}$, then $\lambda b \sqrt{\|\mu\|_\infty} = \tilde{b} \sqrt{L} \sqrt{\|\mu\|_\infty}$, for $\tilde{b}(k_1, k_2) > 0$. The constants b and \tilde{b} could be determined via computer simulation.

Theorem 2 means that the steady-state differentiation error is proportional to $\sqrt{\|\mu\|_\infty \|u''\|_\infty}$, when the differentiator (3.1) and (3.2) is driven by the noisy measurement $u_{noisy}(t) = u(t) + \mu(t)$, provided the second derivative of $u(t)$ is bounded.

3.2 Arbitrary Order Robust Exact Differentiator

Exact derivatives may be calculated by successive implementation of the robust exact differentiator (3.1), (3.2) and (3.3) with finite time convergence. However, in the presence of noise, the differentiation error for the $(n-1)^{th}$ derivative will be proportional to $\|\mu\|_\infty^{1/2^n}$. Thus, the differentiation accuracy deteriorates rapidly when noise is successively differentiated. It is proved in [24] that if the $(n-1)^{th}$ derivative of $u(t)$ has a Lipschitz's constant L , the best possible differentiation accuracy for the k^{th} derivative, where $1 \leq k \leq n-1$ is proportional to $L^{k/n} \|\mu\|_\infty^{(1-k/n)}$. Therefore, a special differentiator is to be designed for each differentiation order. In [25] A. Levant proposed two similar recursive schemes for designing an n^{th} order differentiator that is exact in the absence of noise and provides for an error bound of the order $O(L^{k/n} \|\mu\|_\infty^{(1-k/n)})$, for $1 \leq k \leq n-1$ in the presence of noise, when the k^{th} derivative of $u(t)$ is estimated. Let an n^{th} -order differentiator $D_{n-1}(u_{noisy}(\cdot), L)$ produce outputs $D_{n-1}^k(u_{noisy})$, for $0 \leq k \leq n-1$, being estimations of $u, u', \dots, u^{(n-1)}$, where the $(n-1)^{th}$ derivative of u has a Lipschitz's constant $L > 0$. Then the $(n+1)^{th}$ -order differentiator with outputs $z_k = D_n^k(u_{noisy})$, $0 \leq k \leq n$, being estimates of

$u, u', \dots, u^{(n)}$ is defined as

$$\begin{aligned}
\dot{z}_0 &= \nu, \quad \nu = -\lambda_0 \left| z_0 - u_{noisy}(t) \right|^{(n-1)/n} \text{sign}(z_0 - u_{noisy}(t)) + z_1, \\
z_1 &= D_{n-1}^0(\nu(\cdot), L), \\
&\vdots \\
z_n &= D_{n-1}^{n-1}(\nu(\cdot), L),
\end{aligned} \tag{3.4}$$

where the base differentiator $D_1(u(\cdot), L)$ is a non-linear filter

$$D_1 : \dot{z} = -\lambda \text{sign}(z - u_{noisy}(t)), \quad \lambda > L \tag{3.5}$$

The second-order differentiator resulting from scheme (3.4) and (3.5) is

$$\begin{aligned}
\dot{z}_0 &= \nu, \quad \nu = -\lambda_0 \left| z_0 - u_{noisy}(t) \right|^{1/2} \text{sign}(z_0 - u_{noisy}(t)) + z_1, \\
\dot{z}_1 &= -\lambda_1 \text{sign}(z_1 - u_{noisy}(t)) = -\lambda_1 \text{sign}(z_0 - u_{noisy}(t)),
\end{aligned} \tag{3.6}$$

Another recursive scheme is based on the differentiator (3.6) as a base one. Two additional states are introduced with this scheme for each consecutive derivative. To estimate the k^{th} derivative, for $0 \leq k \leq n$, an observer of the order $2n$ is constructed. Let $\tilde{D}_{2(n-1)}(u_{noisy}, L)$ provide estimates of $u, u', \dots, u^{(n-1)}$, and L is the Lipschitz constant for $u^{(n-1)}$ where $\tilde{D}_2(u_{noisy}, L)$ coincides with (3.6), then $\tilde{D}_{2n}(u_{noisy}, L)$ is defined as

$$\begin{aligned}
\dot{z}_0 &= \nu, \\
\nu &= -\lambda_0 |z_0 - u_{noisy}(t)|^{n/(n+1)} \text{sign}(z_0 - u_{noisy}(t)) + z_1 + w_0, \\
\dot{w}_0 &= -\alpha_0 |z_0 - u_{noisy}(t)|^{(n-1)/(n+1)} \text{sign}(z_0 - u_{noisy}(t)), \\
z_1 &= \tilde{D}_{2(n-1)}^0(\nu(\cdot), L), \\
&\vdots \\
z_n &= \tilde{D}_{2(n-1)}^{n-1}(\nu(\cdot), L),
\end{aligned} \tag{3.7}$$

The 4th order differentiator that estimates the first and second derivative, resulting from scheme (3.6) and (3.7) [27] is

$$\begin{aligned}
z_0 &= \nu_0, \quad \nu_0 = -\lambda_0 |z_0 - u_{noisy}(t)|^{2/3} \text{sign}(z_0 - u_{noisy}(t)) + z_1 + w_0, \\
\dot{w}_0 &= -\alpha_0 |z_0 - u_{noisy}(t)|^{1/3} \text{sign}(z_0 - u_{noisy}(t)), \\
\dot{z}_1 &= \nu_1, \quad \nu_1 = -\lambda_1 |z_1 - \nu_0|^{1/2} \text{sign}(z_1 - \nu_0) + w_1, \\
\dot{w}_1 &= -\alpha_1 \text{sign}(z_1 - \nu_0); \quad z_2 = w_1.
\end{aligned} \tag{3.8}$$

Similarly, an arbitrary order differentiator could be taken as a base one. If the base differentiator is of order m , the differentiator that estimates the derivatives lower than or equal to n would be of order mn . Whereas A. Levant checked the schemes (3.6), (3.4) and (3.8), (3.7), the conjecture is that all such schemes produce working differentiators, provided suitable parameter choice.

Differentiator (3.6), (3.4) could be written as

$$\begin{aligned}
\dot{z}_0 &= \nu_0, \quad \nu_0 = -\lambda_0 \left| z_0 - u_{noisy}(t) \right|^{n/(n+1)} \text{sign}(z_0 - u_{noisy}(t)) + z_1, \\
\dot{z}_1 &= \nu_1, \quad \nu_1 = -\lambda_0 \left| z_1 - \nu_0 \right|^{(n-1)/n} \text{sign}(z_1 - \nu_0) + z_2, \\
&\vdots \\
\dot{z}_{n-1} &= \nu_{n-1}, \quad \nu_{n-1} = -\lambda_{n-1} \left| z_{n-1} - \nu_{n-2} \right|^{1/2} \text{sign}(z_{n-1} - \nu_{n-2}) + z_n, \\
\dot{z}_n &= -\lambda_n \text{sign}(z_n - \nu_{n-1}),
\end{aligned} \tag{3.9}$$

or eliminating the variables $\nu_0, \nu_1, \dots, \nu_{n-1}$ as

$$\begin{aligned}
\dot{z}_0 &= -k_0 \left| z_0 - u_{noisy}(t) \right|^{n/(n+1)} \text{sign}(z_0 - u_{noisy}(t)) + z_1, \\
\dot{z}_i &= -k_i \left| z_0 - u_{noisy}(t) \right|^{(n-i)/(n+1)} \text{sign}(z_0 - u_{noisy}(t)) + z_{i+1}, \\
i &= 1, \dots, n-1 \\
\dot{z}_n &= -k_n \text{sign}(z_0 - u_{noisy}(t)),
\end{aligned} \tag{3.10}$$

where k_0, k_1, \dots, k_n are calculated on the basis of $\lambda_0, \lambda_1, \dots, \lambda_n$.

Theorem 3 *In the absence of input noise ($\mu(t) \equiv 0$), if the parameters λ_i, α_i , are properly chosen, the following equalities hold after a finite time transient process*

$$z_0 = u(t); \quad z_i = \nu_{i-1} = u^{(i)}(t), \quad i = 1, \dots, n.$$

Theorem 4 *Let the input noise satisfy $\|\mu\|_\infty < \infty$. Then the following inequalities hold after finite transient time for some $b_i(\lambda_i, \alpha_i) > 0$*

$$\left| z_i(t) - u^{(i)}(t) \right| \leq b_i \|\mu\|_\infty^{(n-i+1)/(n+1)}, \quad i = 0, \dots, n.$$

The parameters λ_i, α_i , are to be chosen recursively such that $\lambda_1, \alpha_1, \dots, \lambda_n, \alpha_n$, provide for the convergence of the differentiator producing derivatives up to $(n - 1)^{th}$, Lipschitz's constant L , and λ_0, α_0 , are sufficiently large, where α_0 is chosen first. The best way is to choose them by computer simulation.

Proposition 1 *Let parameters $\alpha_{0i}, \lambda_{0i}, i = 0, \dots, n$ of differentiators (3.6), (3.4) or (3.8), (3.7) provide for exact n^{th} -order differentiation with $L=1$, in the absence of measurement noise. Then the parameters $\alpha_i = \alpha_{0i}L^{2/(n-i+1)}$, $\lambda_i = \lambda_{0i}L^{1/(n-i+1)}$ are valid for any $L > 0$ and provide for the accuracy*

$$\left| z_i(t) - u^{(i)}(t) \right| \leq \tilde{b}_i L^{i/(n+1)} \|\mu\|_{\infty}^{(n-i+1)/(n+1)}, \quad i = 0, \dots, n, \quad (3.11)$$

where $\tilde{b}_i(\lambda_{0i}, \alpha_{0i}) \geq 1$.

Proposition 1 allows for tabulating the parameters $\alpha_{0i}, \lambda_{0i}, i = 0, \dots, n$, which would enable convenient design of the differentiators for arbitrary $L > 0$. A. Levant provides the values for $\lambda_{00}, \lambda_{01}, \dots, \lambda_{05}$, for the scheme (3.6), (3.4). The differentiator with the parameters $\lambda_{00}, \lambda_{01}, \dots, \lambda_{05}$, provides estimates of $u, u', \dots, u^{(5)}$, for u such that $u^{(5)}$ has a Lipschitz's constant $L = 1$. For $k < n$, the parameters for a k^{th} -order differentiator coincide with the last k parameters of an n^{th} -order differentiator; that is $\lambda_{0k} = \lambda_{0n}, \lambda_{0k-1} = \lambda_{0n-1}, \dots, \lambda_{00} = \lambda_{0n-k}$.

3.3 In Comparison to High-Gain Observers

In Table 3.1 we list the features of high-gain observers and robust exact differentiators side by side. To design a high-gain observer (2.2) to produce outputs that

approximate the k^{th} , $1 \leq k \leq n - 1$, derivatives of an input $u(\cdot)$ under ideal conditions with no measurement noise, the n^{th} derivative of $u(\cdot), u^{(n)}(\cdot)$ needs to be bounded. Since the differentiation error is ultimately bounded by (2.9)

$$\delta + \varepsilon^{n-k+1} \|u^{(n)}\|_{\infty} \int_0^{\infty} |\{exp(A\eta\tau)B\}_k| d\tau,$$

for $1 \leq k \leq n - 1$ and δ arbitrarily small, to ensure that the error is within a given tolerance one needs to know $\|u^{(n)}\|_{\infty}$. To ensure the convergence of the outputs of the robust exact differentiator (3.6), (3.4) to $u(\cdot), u'(\cdot), \dots, u^{(n-1)}(\cdot)$, knowledge of the Lipschitz's constant of the $(n-1)^{th}$ derivative of the input $u(\cdot)$ is necessary. If $u^{(n-1)}$ is differentiable and $u^{(n)}$ is bounded, the Lipschitz's constant of the $(n-1)^{th}$ derivative of $u(\cdot)$ is equal to $\|u^{(n)}\|_{\infty}$.

In the presence of noise, if the ratio $\|u^{(n)}\|_{\infty}/\|\mu\|_{\infty}$ is known, it is possible to choose the parameter ε of the high-gain observer (2.2), such that the differentiation error is of the same order as the differentiation error of the robust exact differentiator (3.6) and (3.8), which is the smallest possible order as proved by A. Levant [24]. The bound on the differentiation error in the presence of noise for the high-gain observer is given by (2.12). We provide the constants P_k and Q_k , for high-gain observers of order less than or equal to 10 tabulated in an Appendix which makes computing the error bound easy provided $\|u^{(n)}\|_{\infty}$ and $\|\mu\|_{\infty}$ are known. For the sliding mode observer the differentiation error is bounded by (3.11). The constants $\tilde{b}_i(\lambda_{0i}, \alpha_{0i})$ could be estimated via simulation for a particular choice of the parameters $\lambda_{0i}, \alpha_{0i}$.

In the presence of noise when an n^{th} order high-gain observer is used to differentiate a signal $u(\cdot)$, the ratio between the bound on the n^{th} derivative of $u(\cdot)$ and the bound on the magnitude of the noise needs to be known in order to ensure that the bound on the differentiation error is of the smallest possible order

as given by (2.12).

In the absence of noise, reducing the high-gain observer parameter ε in (2.2) will ensure the convergence of the outputs of the observer to the vicinity of the derivatives of its input if the n^{th} derivative of the input is bounded regardless of the size of the bound on $u^{(n)}(\cdot)$, $\|u^{(n)}\|_\infty$. To insure the convergence of the outputs of the sliding-mode observer to the derivatives of the input it is necessary to know the Lipschitz's constant of the highest estimated derivative (which coincides with $\|u^{(n)}\|_\infty$ when $u^{(n-1)}$ has a bounded derivative) prior to the design. The design of the sliding-mode differentiator (3.6) and (3.8) is independent of the bound on the noise $\|\mu\|_\infty$ and the error bound is of the smallest possible order as in (3.11).

Table 3.1: A comparative summary of the features of high-gain observers versus robust exact differentiators developed by A. Levant

Feature	High-Gain Observers	Robust Exact Differentiators
Complexity	Linear; we tabulated the constants necessary to make the design straightforward	Nonlinear; a system with differential equations with discontinuous right-hand side
Accuracy in the absence of noise	The observer could be designed such that the differentiation error is arbitrarily small after finite time	The differentiation error is zero after transient time
Accuracy in the presence of noise	The differentiation error is proportional to $\ u^{(n)}\ _{\infty}^{k/n} \ \mu\ _{\infty}^{(n-k)/n}$, where u is the signal to be differentiated, $u^{(n)}$ is the n^{th} derivative of the signal u , n is the order of the observer, k is the estimated derivative ($1 \leq k \leq n - 1$) and μ is uniformly bounded noise.	The differentiation error is proportional to $L^{k/n} \ \mu\ _{\infty}^{(n-k)/n}$, where u is the signal to be differentiated, L is the Lipschitz's constant of the $(n - 1)^{th}$ derivative, k is the estimated derivative, ($0 \leq k \leq n - 1$) and μ is uniformly bounded noise.
Computability of the bound	We provide an algorithm to compute the bound given $\ u^{(n)}\ _{\infty}$ and $\ \mu\ _{\infty}$	The bound could be estimated via simulation
Prior knowledge needed for the design in the absence of noise	The quantity $\ u^{(n)}\ _{\infty}$	The Lipschitz's constant of the highest estimated derivative
Prior knowledge needed for the design in the presence of noise	The ratio $\ u^{(n)}\ _{\infty} / \ \mu\ _{\infty}$	The Lipschitz's constant of the highest estimated derivative

3.4 Computer Simulation

In this section we compare robust exact differentiators developed by A. Levant and high-gain observers via simulation. The simulation was carried out via MATLAB and SIMULINK. The noise used throughout the simulation is always a rescaled version of noise shown in Figure 2.7. First we examine the error while differentiating sinusoids of various frequencies contaminated with white noise of varied magnitude using high-gain observer and higher-order sliding-mode robust, exact differentiator. We then compare the performance of higher-order sliding-mode differentiators to high-gain observers on more complex signals. The high-gain parameter ε is always chosen such that the error bound (2.12) is minimized as described in Chapters 2 and 3.

To differentiate sinusoids we used the 6th-order sliding-mode robust, exact differentiator estimating up to the 5th derivative given by the equations (3.12)

$$\begin{aligned}
 \dot{z}_0 &= \nu_0, \quad \nu_0 = -12L^{1/6} |z_0 - u_{noisy}(t)|^{5/6} \text{sign}(z_0 - u_{noisy}(t)) + z_1, \\
 \dot{z}_1 &= \nu_1, \quad \nu_1 = -8L^{1/5} |z_1 - \nu_0|^{4/5} \text{sign}(z_1 - \nu_0) + z_2, \\
 \dot{z}_2 &= \nu_2, \quad \nu_2 = -5L^{1/4} |z_2 - \nu_1|^{3/4} \text{sign}(z_2 - \nu_1) + z_3, \\
 \dot{z}_3 &= \nu_3, \quad \nu_3 = -3L^{1/3} |z_3 - \nu_2|^{2/3} \text{sign}(z_3 - \nu_2) + z_4, \\
 \dot{z}_4 &= \nu_4, \quad \nu_4 = -1.5L^{1/2} |z_4 - \nu_3|^{1/2} \text{sign}(z_4 - \nu_3) + z_5, \\
 \dot{z}_5 &= -1.1L \text{sign}(z_5 - \nu_4),
 \end{aligned} \tag{3.12}$$

where $u_{noisy}(t) = A \sin(\omega t) + \mu(t)$, $\mu(t)$ is white noise and $L = A\omega^6$ is the Lipschitz's constant for the 5th derivative of the differentiated sinusoid of amplitude

A and frequency ω . The 6^{th} -order high-gain observer is given by (3.13).

$$\begin{aligned}
 \dot{\hat{x}}_1 &= -\frac{\alpha_1}{\varepsilon}(\hat{x}_1 - u_{noisy}) + \hat{x}_2, \\
 \dot{\hat{x}}_2 &= -\frac{\alpha_2}{\varepsilon^2}(\hat{x}_2 - u_{noisy}) + \hat{x}_3, \\
 \dot{\hat{x}}_3 &= -\frac{\alpha_3}{\varepsilon^3}(\hat{x}_3 - u_{noisy}) + \hat{x}_4, \\
 \dot{\hat{x}}_4 &= -\frac{\alpha_4}{\varepsilon^4}(\hat{x}_4 - u_{noisy}) + \hat{x}_5, \\
 \dot{\hat{x}}_5 &= -\frac{\alpha_5}{\varepsilon^5}(\hat{x}_5 - u_{noisy}) + \hat{x}_6, \\
 \dot{\hat{x}}_6 &= -\frac{\alpha_6}{\varepsilon^6}(\hat{x}_6 - u_{noisy}).
 \end{aligned} \tag{3.13}$$

Figure 3.1 displays the sliding-mode and high-gain estimate of the first and second derivative of a sinusoid contaminated by white noise with magnitude no higher than 0.01. Tables 3.2-3.9 display the estimation error for higher-order sliding-mode differentiator and high-gain observer. The error was computed as $\max_{t \geq T} |u^{(k)}(t) - \hat{x}_{k+1}(t)|$ (or $z_k(t)$), where t is time and $T = 4$ seconds is transient time. The performance of high-gain observer and higher-order sliding-mode observer is comparable.

Table 3.2: The percentage differentiation error for a 6^{th} order high-gain observer and a 6^{th} order HOSM differentiator. The differentiated signal is $\sin(t)$ and $\|\mu\|_\infty = 0.01$.

Derivative	High-Gain Observer	HOSM Observer
1^{st}	4.11 %	3.15 %
2^{nd}	25.10 %	27.45 %
3^{rd}	81.62 %	103.70 %
4^{th}	151.59 %	150.96 %
5^{th}	151.03 %	115.47 %

Observe from Tables 3.2-3.6 that the estimates for derivatives higher than the second derivative are useless for the lower noise level of $\|\mu\|_\infty = 0.01$. Observe too that the high-gain observer outperforms the sliding-mode observer for high

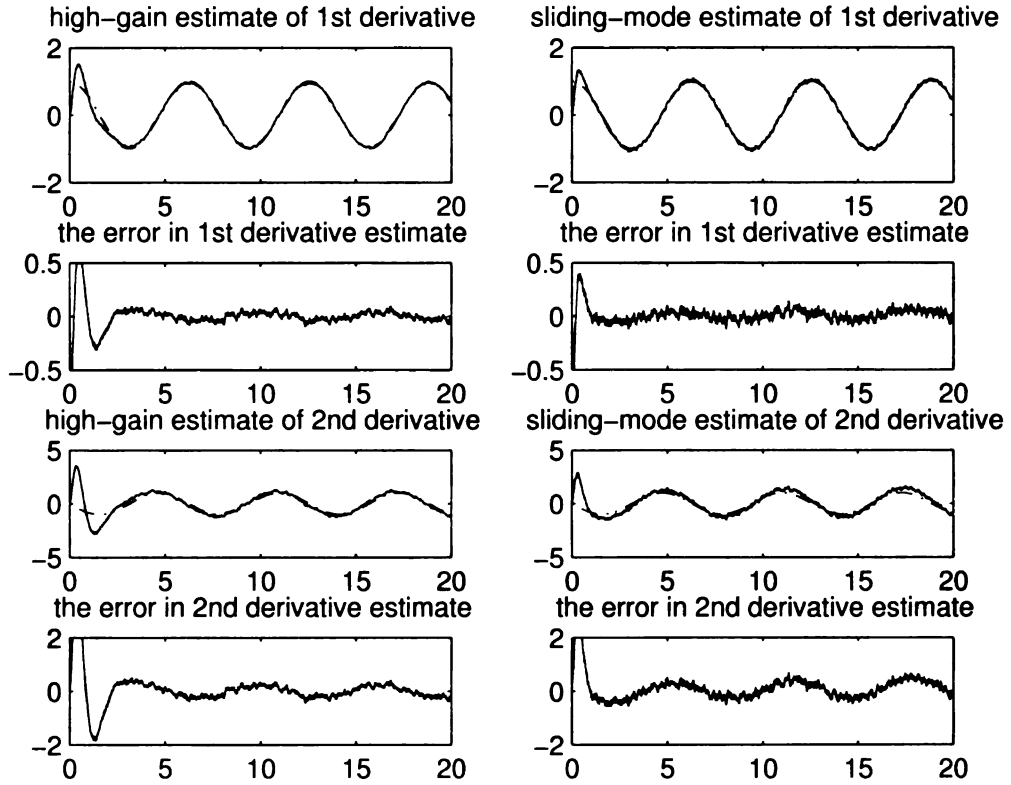


Figure 3.1: Sliding-mode/high-gain estimate of first and second derivative of a noisy sinusoid.

frequency sinusoids, whereas the sliding-mode observer outperforms the high-gain observer for low-frequency sinusoids. Tables 3.7-3.9 indicate that it is pointless to estimate derivatives beyond first for the higher noise level of $\|\mu\|_\infty = 0.1$. For both, high-gain observer and sliding mode observer part of the error is due to a phase shift of the estimate with respect to the actual derivative as Figure (3.2) shows. Note that even though in Tables 3.7-3.9 the magnitude of the noise is 10 times the magnitude of the noise in Tables 3.2-3.6 the error bound (2.15) for corresponding signals increases by a factor of $10^{\frac{6-k}{6}}$, where k is the order of the derivative. For the fifth derivative $k = 5$, and $10^{\frac{6-k}{6}} = 1.46$. This means that we may reasonably expect the error for the 5th derivative estimated with high-gain observer in Table 3.9 where the magnitude of the noise is 0.1 to be

Table 3.3: The percentage differentiation error for a 6th order high-gain observer and a 6th order HOSM differentiator. The differentiated signal is $\sin(0.5t)$ and $\|\mu\|_\infty = 0.01$.

Derivative	High-Gain Observer	HOSM Observer
1 st	5.98 %	2.6 %
2 nd	36.7 %	23.6 %
3 rd	116.88 %	94.4 %
4 th	198.24 %	147.2 %
5 th	150.48 %	114.7 %

Table 3.4: The percentage differentiation error for a 6th order high-gain observer and a 6th order HOSM differentiator. The differentiated signal is $\sin(5t)$ and $\|\mu\|_\infty = 0.01$.

Derivative	High-Gain Observer	HOSM Observer
1 st	5.2 %	5.05 %
2 nd	28.4 %	38.06 %
3 rd	88.6 %	121.63 %
4 th	156.2 %	176.6 %
5 th	153 %	122.5 %

1.46 times the error for the 5th derivative estimated with high-gain observer in Table 3.5 where the noise magnitude is 0.01; however, the error is comparable. In this simulation we took the high-gain parameter ε as $\varepsilon = \frac{\sum_{k=1}^5 \varepsilon_k^{opt}}{5}$. Perhaps this causes the error to be closer to the error bound in the case of noise μ with $\|\mu\|_\infty = 0.01$.

Next, we compare the higher-order sliding-mode and high-gain observer on the signal (3.14).

$$u = y - [10\sin(0.05x) + 5], \quad (3.14)$$

Table 3.5: The percentage differentiation error for a 6th order high-gain observer and a 6th order HOSM differentiator. The differentiated signal is $\sin(10t)$ and $\|\mu\|_\infty = 0.01$.

Derivative	High-Gain Observer	HOSM Observer
1 st	5.6 %	8.3 %
2 nd	30.3 %	51.76 %
3 rd	93.18 %	139.65 %
4 th	160.2 %	180.9 %
5 th	155.95 %	124.04 %

Table 3.6: The percentage differentiation error for a 6th order high-gain observer and a 6th order HOSM differentiator. The differentiated signal is $\sin(50t)$ and $\|\mu\|_\infty = 0.01$.

Derivative	High-Gain Observer	HOSM Observer
1 st	8.4 %	13.63 %
2 nd	40.4 %	74.3 %
3 rd	110.6 %	188.8 %
4 th	178.1 %	222.4 %
5 th	162.7 %	142.13 %

where x and y are the states of the system

$$\dot{x} = \nu \cos\varphi,$$

$$\dot{\varphi} = \frac{\nu}{5} \tan\theta,$$

$$\dot{\theta} = c,$$

$$\dot{y} = \nu \sin\varphi,$$

$$c = -20 \operatorname{sign}\{u^{(3)} + 3(\ddot{u}^6 + \dot{u}^4 + |u|^3)^{1/12} \times \operatorname{sign}[\ddot{u} + (\dot{u}^4 + |u|^3)^{1/6} \times \operatorname{sign}(\dot{u} + 0.5|u|^{3/4} \operatorname{sign}(u))]\},$$

We differentiated the aforementioned signal $u_{noisy}(t) = u(t) + \mu(t)$, using a 3rd order high-gain observer with multiple real eigenvalues and a 3rd order sliding-

Table 3.7: The percentage differentiation error for a 6th order high-gain observer and a 6th order HOSM differentiator. The differentiated signal is $\sin(0.1t)$ and $\|\mu\|_\infty = 0.1$.

Derivative	High-Gain Observer	HOSM Observer
1 st	66.9 %	17.5 %
2 nd	269 %	99 %
3 rd	340 %	140 %
4 th	317 %	147.05 %
5 th	857 %	814 %

Table 3.8: The percentage differentiation error for a 6th order high-gain observer and a 6th order HOSM differentiator. The differentiated signal is $\sin(t)$ and $\|\mu\|_\infty = 0.1$.

Derivative	High-Gain Observer	HOSM Observer
1 st	20.48 %	14.45 %
2 nd	78.62 %	68.67 %
3 rd	173.10 %	165.65 %
4 th	205.97 %	163.47 %
5 th	143.29 %	109.05 %

mode observer given by equations (3.15) [25],

$$\begin{aligned}
 \dot{z}_0 &= \dot{\nu}_0, \nu_0 = -3L^{1/3}|z_0 - u|^{2/3} \operatorname{sign}(z_0 - u) + z_1, \\
 \dot{z}_1 &= \nu_1, \nu_1 = -1.5L^{1/2}|z_1 - \nu_0|^{1/2} \operatorname{sign}(z_1 - \nu_0) + z_2, \\
 \dot{z}_2 &= -1.1L \operatorname{sign}(z_1 - \nu_1),
 \end{aligned} \tag{3.15}$$

where $L = \|u^{(3)}\|_\infty = 6$. We added white noise $\mu(t)$ such that $\|\mu\|_\infty = 0.012$. For the 3rd order high-gain observer with multiple real eigenvalues, $\varepsilon_1^{opt} = 0.0836$ and $\varepsilon_2^{opt} = 0.0939$. In the simulation we set $\varepsilon = (\varepsilon_1^{opt} + \varepsilon_2^{opt})/2 = 0.0887$. Figure (3.3) displays the estimates and estimation errors of the first and second derivatives of $u(t)$ with high-gain observer and sliding-mode observer. The steady-state error

Table 3.9: The percentage differentiation error for a 6th order high-gain observer and a 6th order HOSM differentiator. The differentiated signal is $\sin(10t)$ and $\|\mu\|_\infty = 0.1$.

Derivative	High-Gain Observer	HOSM Observer
1 st	28.25 %	42.59 %
2 nd	96.2823 %	149.5259 %
3 rd	194.48 %	265.36 %
4 th	229.02 %	212.32 %
5 th	151.70 %	121.63 %

for the first derivative after 3 seconds is 0.1361 for the high-gain observer and 0.1408 for the sliding-mode observer. For the second derivative, the steady-state error after 3 seconds is 1.4655 for the high-gain observer and 1.2497 for the sliding-mode observer. However, for a 3rd order high-gain observer with $\varepsilon = 0.05$, the steady-state error after 3 seconds is 0.0714 in the estimate of the first derivative, and 1.0051 in the estimate of the second derivative.

We now differentiate the signal $u_1(t)$ being the state $x_1(t)$ of the 3rd order nonlinear system.²

$$\begin{bmatrix} \dot{x}_1 \\ \dot{x}_2 \\ \dot{x}_3 \end{bmatrix} = \begin{bmatrix} 0 & 1 & 0 \\ 0 & 0 & 1 \\ 0 & 0 & 0 \end{bmatrix} \begin{bmatrix} x_1 \\ x_2 \\ x_3 \end{bmatrix} + \begin{bmatrix} 0 \\ 0 \\ 1 \end{bmatrix} b(x_1, x_2, x_3),$$

$$u = x_1,$$

$$b(x_1, x_2, x_3) = \alpha(x_1, x_2, x_3)g_s(x_1, x_2, x_3) + (1 - \alpha(x_1, x_2, x_3))g_u(x_1, x_2, x_3),$$

$$\alpha(x_1, x_2, x_3) = 2 \frac{x_1^2 + x_2^2 + x_3^2}{1 + x_1^2 + x_2^2 + x_3^2},$$

$$g_s(x_1, x_2, x_3) = -54x_1 - 36x_2 - 9x_3,$$

$$g_u(x_1, x_2, x_3) = 54x_1 - 36x_2 + 9x_3,$$

(3.16)

²System (3.16) was used in [10] to test a numerical differentiator.

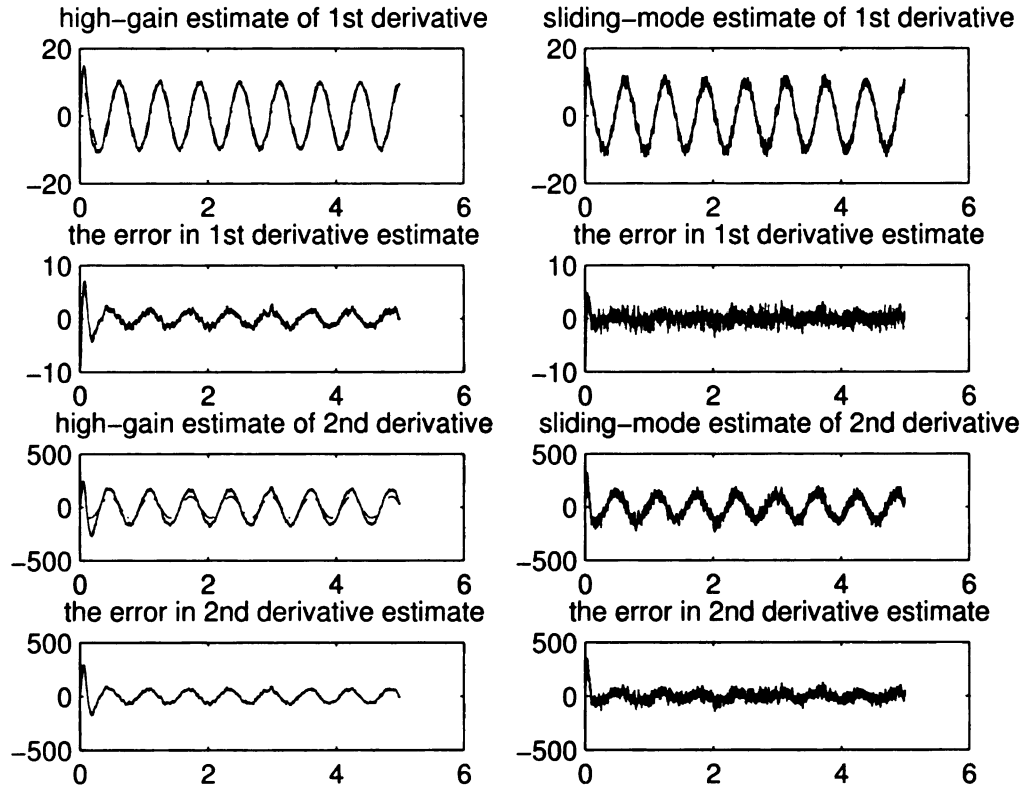


Figure 3.2: The estimate of derivatives of $\sin(10t) + \mu(t)$ with high-gain/sliding-mode observer. The noise magnitude is $\|\mu\|_\infty = 0.1$.

The differentiator (3.15) and a 3^{rd} order high-gain observer with multiple real eigen-values were used. It was observed from simulation that the 3^{rd} derivative of u_1 is bounded by 16, the parameter ε was set as $\varepsilon = 0.064$. The noise is bounded by 0.012. Figure (3.4) shows the estimate of first and second derivatives with a sliding-mode observer and high-gain observer. The estimation error for the first derivative is 0.1 for high-gain observer and 0.12 for the sliding-mode observer, whereas for the second derivative the estimation error is 1.7 for the high-gain observer and 1.73 for the sliding-mode observer.

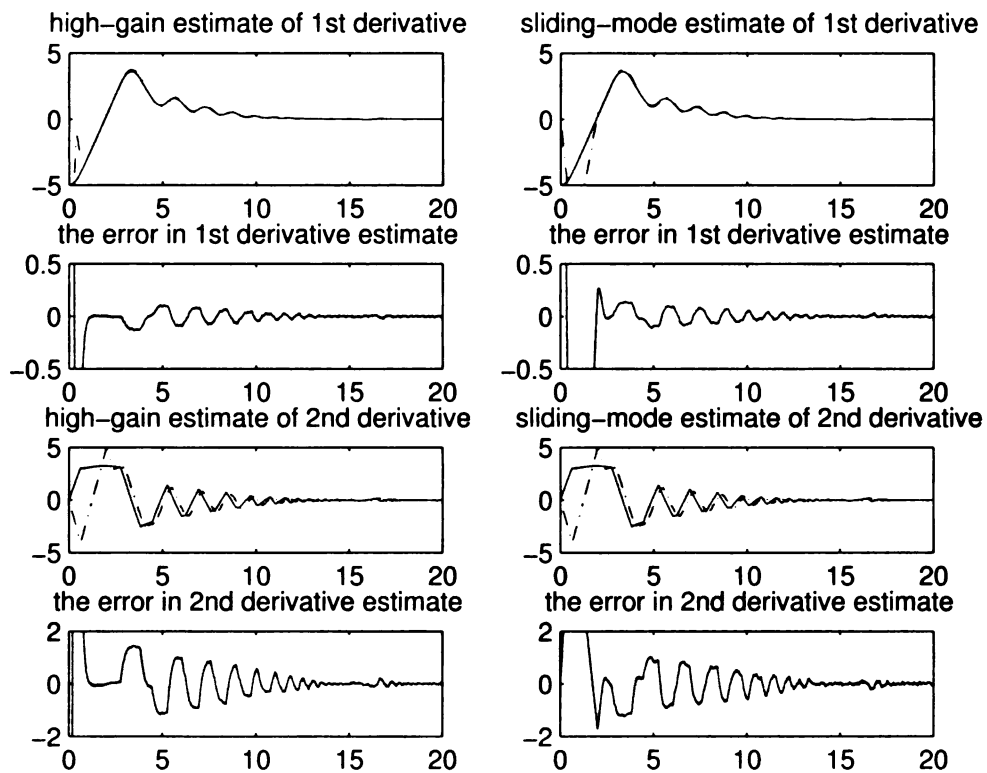


Figure 3.3: The estimate of derivatives of (3.14) with high-gain/sliding-mode observer. The solid line depicts the actual derivative, whereas the dashed line is the estimate.

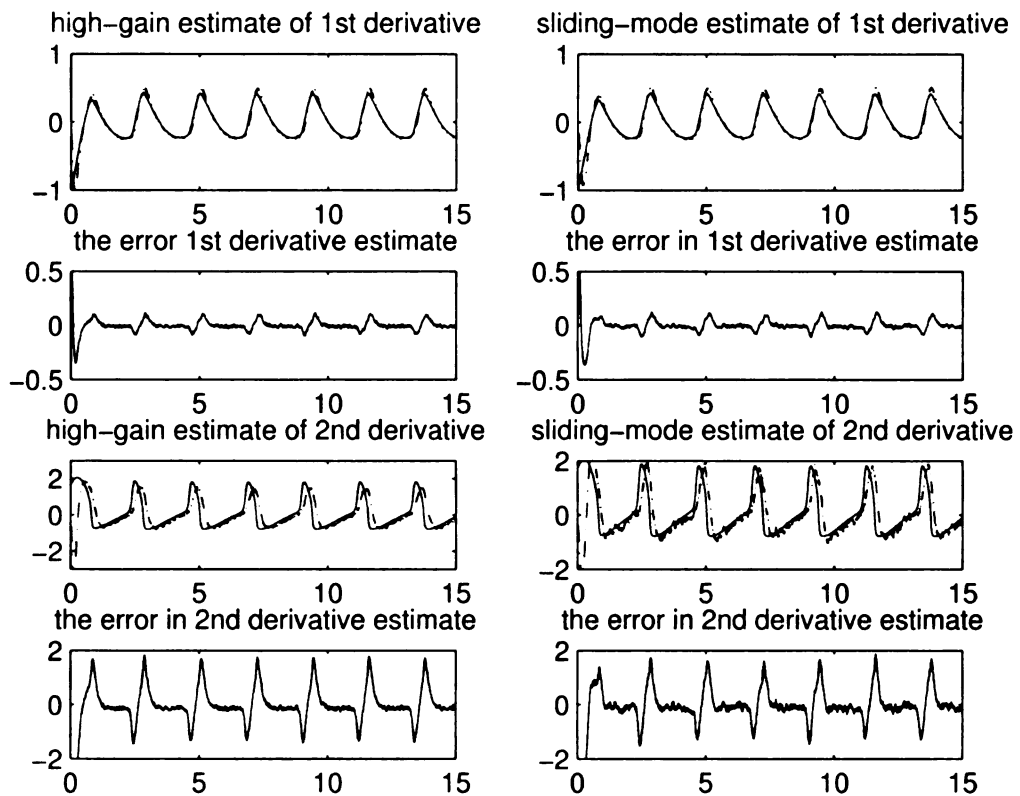


Figure 3.4: Sliding-mode/high-gain estimate of the derivatives of u_1 given by (3.16). The solid line depicts the actual derivative, whereas the dashed line is the estimate.

Chapter 4

Conclusions

The theory of high gain observers is an asymptotic theory. Ideally, when no measurement noise is present the estimation error shrinks to zero as the gain of the observer grows to infinity. When noise is present, the high-gain of the observer amplifies the noise. Hence, in the presence of noise there is a trade-off between the error in the absence of noise and the amplification of the noise. The trade-off is quantified through the ratio of a uniform bound on the noise and a uniform bound on the n^{th} derivative of the differentiated signal, where n is the order of the observer. Due to this trade-off, when the high-gain observer is used for differentiation, extra care is to be taken when designing the gain. The gain should be neither too large, nor too small. We find that the gain of an n^{th} order observer should be of the order $O\left(\frac{\|u^{(n)}\|_{\infty}}{\|\mu\|_{\infty}}\right)$.

Inspired by Levant's results in [25, 24, 26], where Levant showed that a numerical differentiator can not provide for accuracy better than $O(L^{i/n}\|\mu\|_{\infty}^{(n-i)/n})$, and developed differentiators that provide for this accuracy, we showed that the high-gain observer can provide for this same accuracy if the gain is properly chosen. First, we showed that the estimation error when high-gain observer is used as

a differentiator is bounded by

$$b_k(\varepsilon) \equiv \delta + P_{k+1} \|u^{(n)}\|_\infty \varepsilon^{n-k} + \frac{Q_{k+1} \|\mu\|_\infty}{\varepsilon^k},$$

where k is the estimated derivative, n is the order of the observer, P_k, Q_k are constants dependent on the order and eigenvalues of the observer, and δ could be made arbitrarily small. The effect of the order and the choice of eigenvalues on the estimation error is analyzed in Chapter 2. We provide the constants $P_k, Q_k, 1 \leq k \leq n$ and $n = 1, 2, \dots, 10$ for high-gain observer with multiple real eigenvalues in Appendix 1 of this thesis.

Next, we choose

$$\varepsilon_k^{opt} = \sqrt[n]{\frac{k}{n-k}} \sqrt[n]{\frac{Q_{k+1} \|\mu\|_\infty}{P_{k+1} \|u^{(n)}\|_\infty}},$$

that minimizes the error bound $b_k(\varepsilon)$. Note that, the choice of ε depends on the derivative estimated. However, we observed during simulation that ε_k^{opt} does not vary significantly with k , nor does $b_k(\varepsilon)$ vary significantly with ε , which allowed us to choose $\varepsilon = \frac{\sum_{k=1}^n \varepsilon_k^{opt}}{n}$ throughout the simulation. It is important to realize that this choice of ε_k^{opt} minimizes the error bound on the estimation error for a class of signals u with the same $\|u^{(n)}\|_\infty$, rather than the error for the particular signal at hand. In Lemma 1 we show that there is a signal for which the estimation error comes arbitrarily close to the bound $b_k(\varepsilon)$. Simulation examples are presented to verify and clarify analytical results.

In Chapter 3 we compare high-gain observers to Levant's sliding-mode differentiators. Table 3.1 is a comparative summary of the features of high-gain observers and sliding-mode differentiators. Simulation shows that in the presence of noise the performance of high-gain observers and sliding-mode observers is com-

parable. It appears that high-gain observers are better for high frequency signals, whereas sliding-mode observers are better for low frequency signals. The signal to noise ratio ¹ affects the usefulness of the estimated derivatives. In our examples, the error for estimates of 3rd and higher derivatives was over 50%, making the estimates useless for both of the observers. We also observed from simulation examples that large portion of the error is due to a phase shift of the estimate from the actual derivative. Also, being a low-pass filter, the high-gain observer deminishes the high-frequency components of the noise.

Results in this thesis for high-gain observers, as well as results in [25, 24, 26] for sliding-mode differentiators outline the limitations on differentiation in the presence of noise. They also provide design guidelines to achieve best results within these limitations. They allow us to quantify the effect of noise on the estimation error, without placing restrictive assumptions on the noise nor on the differentiated signal. The only assumption on the noise is that it is bounded and the bound is known. For the differentiated signal, we require that the bound on the derivative consecutive to the one we wish to estimate is known. However, large measurement noise remains a problem for on-line, real-time differentiation when estimating higher derivatives as simulation examples in Chapter 3 show.

¹By signal to noise ratio, we mean $\frac{\text{infinity norm of the signal}}{\text{infinity norm of the noise}}$

Appendix — Constants

Table 1: The constants P_k for $2 \leq k \leq n$, $2 \leq n \leq 10$ for multiple real eigenvalues

n/k	2	3	4	5	6	7	8	9	10
2	2	0	0	0	0	0	0	0	0
3	3	3	0	0	0	0	0	0	0
4	4	6	4	0	0	0	0	0	0
5	5	10	10	5	0	0	0	0	0
6	6	15	20	15	6	0	0	0	0
7	7	21	35	35	21	7	0	0	0
8	8	28	56	70	56	28	8	0	0
9	9	36	84	126	126	84	36	9	0
10	10	45	120	210	252	210	120	45	10

Table 2: The constants Q_k for $2 \leq k \leq n$, $2 \leq n \leq 10$ for multiple real eigenvalues

n/k	2	3	4	5	6	7	8	9	10
2	0.735	0	0	0	0	0	0	0	0
3	1.750	0.620	0	0	0	0	0	0	0
4	2.990	2.167	0.559	0	0	0	0	0	0
5	4.410	4.881	2.553	0.521	0	0	0	0	0
6	5.979	8.952	7.094	2.917	0.493	0	0	0	0
7	7.678	14.539	15.494	9.615	3.265	0.471	0	0	0
8	9.493	21.785	29.229	24.316	12.435	3.6	0.454	0	0
9	11.411	30.814	49.925	52.162	35.694	15.544	3.925	0.439	0
10	13.424	41.741	79.338	99.893	85.722	49.897	18.934	4.24	0.426

Bibliography

- [1] M. A. Aizerman & E. S. Pyatnitskii, "Foundation of a theory of discontinuous systems: Part I" *Automation and Remote Control*, Vol. 35, pp. 1066-1079, 1974.
- [2] M. A. Aizerman & E. S. Pyatnitskii, "Foundation of a theory of discontinuous systems: Part II" *Ibid*, Vol. 35, pp. 1242-1262, 1974.
- [3] J. H. Ahrens & H. K. Khalil, "Output Feedback Control Using High-Gain Observers in the Presence of Measurement Noise" *IEEE Trans. on AC*, Vol. 44, pp. 1672-1687, 1999.
- [4] B. Aloliwi, H. K. Khalil, and E. G. Strangas, "Robust speed control of induction motors." *In Proc. American Control Conference*, Albuquerque, NM, 1997. WP16:4.
- [5] B. Aloliwi, H. K. Khalil, and E. G. Strangas, L. Laubinger, J. Miller "Robust tracking controllers for induction motors without rotor position sensor: analysis and experimental results." *IEEE Trans. Automat. Contr.*, 14: 1448-1458, 1999.
- [6] G. Bartolini, A. Ferrara, E. Usai, "Applications of a sub-optimal discontinuous control algorithm for uncertain second order systems," *Int. J. of Robust and Nonlinear Control.*, 7(1997)(4), pp.299-310.
- [7] G. Bartolini, A. Ferrara, E. Usai "Chattering avoidance by second-order sliding mode control," *IEEE Trans. Automat. Control*, 43 (1998) (2), pp. 241-246.
- [8] B. Carlsson, A. Ahlen, M. Stenard, "Optimal Differentiation Based on Stochastic Signal Models," *IEEE Transactions on Signal Processing*, vol. 39(2), 1991.
- [9] A. Dabroom & H. K. Khalil, "Discrete-Time Implementation of High-Gain Observers for Numerical Differentiation," *Int. J. Control*, Vol. 72, pp. 1523-1537, 1999.
- [10] S. Diop & J. W. Grizzle & P. E. Morral & A. Stefanopoulou, "Interpolation and Numerical Differentiation for Observer Design," *ACC*, 1523-1537, 1994.

- [11] S. V. Emelyanov, "Binary systems of automatic control," *Moscow institute of control problems*, (1984)
- [12] S. V. Emelyanov, S. K. Korovin , "Applying the principle of control by deviation to extend the set of possible feedback types ." *Soviet Physics, Doklady*, 26 (1981) (6), pp. 562-574.
- [13] S. V. Emelyanov, S. K. Korovin and L. V. Levantovsky, " Higher order sliding modes in the binary control systems," *Soviet Physics, Doklady*, 31 (1986) (4), pp. 291-293.
- [14] S. V. Emelyanov, S. K. Korovin and L. V. Levantovsky, " Second order sliding modes in controlling uncertain systems," *Soviet Journal of Computing and System Science*, 24 (4), 63-68, 1986.
- [15] S. V. Emelyanov, S. K. Korovin and L. V. Levantovsky, " Drift algorithm in control of uncertain processes," *Problems of Control and Information Theory*, 15 (6), 425-438, 1986.
- [16] S. V. Emelyanov, S. K. Korovin and L. V. Levantovsky, " New class of second order sliding algorithms," *Mathematical Modeling*, 2 (3), 89-100, 1990, in Russian.
- [17] A. F. Filippov, *Differential Equations with Discontinuous Right-Hand Side*, Kluwer, Dordrecht, the Netherlands, 1988.
- [18] L. Fridman, A. Levant, *Sliding Mode Control in Engineering*, Marcel Dekker Inc., 2002.
- [19] T. Kailath, "Detection of Stochastic Processes," *IEEE Transactions on Information Theory*, vol. 44, NO 6, October, 1998.
- [20] T. Kailath, "Linear Filtering Theory," *IEEE Transactions on Information Theory*, March, 1974.
- [21] H. K. Khalil, *High-gain observers in nonlinear feedback control. In H. Nijmeijer and T. I. Fosse, editors New Directions in Nonlinear Observer Design*, volume 244 of *Lecture Notes in Control and Information Sciences*, pages 249-268. Springer, London, 1999.
- [22] H. K. Khalil, *Nonlinear Systems*, Prentice Hall, 3rd ed., 2002.
- [23] L. K. Vasiljevic, H. K. Khalil, *Differentiation with high-gain observers in the presence of measurement noise*, Proc. of 45th IEEE CDC, San Diego, CA, 2006.
- [24] A. Levant, "Robust Exact Differentiation via Sliding Mode Technique" *Automatica*, Vol. 34, 1998.

- [25] A. Levant, "Higher Order Sliding Modes, Differentiation and Output Feedback Control" *International Journal of Control*, Vol. 76, 2003.
- [26] A. Levant, "Sliding Order and Sliding Accuracy in Sliding Mode Control" *International Journal of Control*, Vol. 58(6), 1993.
- [27] A. Levant, "Controlling Output Variables with Higher-Order Sliding Mode" *Proceedings of the European Control Conference*, Karlsruhe, Germany, September, 1993.
- [28] A. Levant, "Arbitrary-order sliding modes with finite time convergence," *Proc. of the 6th IEEE Mediterranean Conference on Control and Systems*, June 9-11, 1998, Alghero, Sardinia, Italy.
- [29] L. V. Levantovsky, "Second order sliding algorithms: their realization," *Dynamics of heterogeneous systems. Materials of the seminar*, 1985, Moscow: The institute of system studies, in Russian.
- [30] L. V. Levantovsky, "Sliding modes with continuous control," *Proc. of the All-Union Scientific-Practical Seminar on Application Experience of Distributed Systems*, 1986, Novokuznezk, U.S.S.R., Vol. I, Moscow, in Russian.
- [31] L. V. Levantovsky, "Sliding modes of high orders and their applications for controlling uncertain processes," *Abstract of Ph. D. thesis, deposited at The Institute of Scientific and Technical Information*, Moscow, in Russian.
- [32] V. Utkin, "Variable structure systems with sliding modes: a survey," *IEEE transactions on automatic control*, 22, 1977.
- [33] V. Utkin, "Sliding modes in optimization and control problems," *Nauka, Moscow* 1981.

MICHIGAN STATE UNIVERSITY LIBRARIES



3 1293 02956 2117